BRITISH GEOLOGICAL SURVEY

Fluid Processes and Waste Management Group

TECHNICAL REPORT WE/98/23

Electrokinetic Sounding Results, INCO-DC Project 950176, Cyprus, 1997

David Beamish

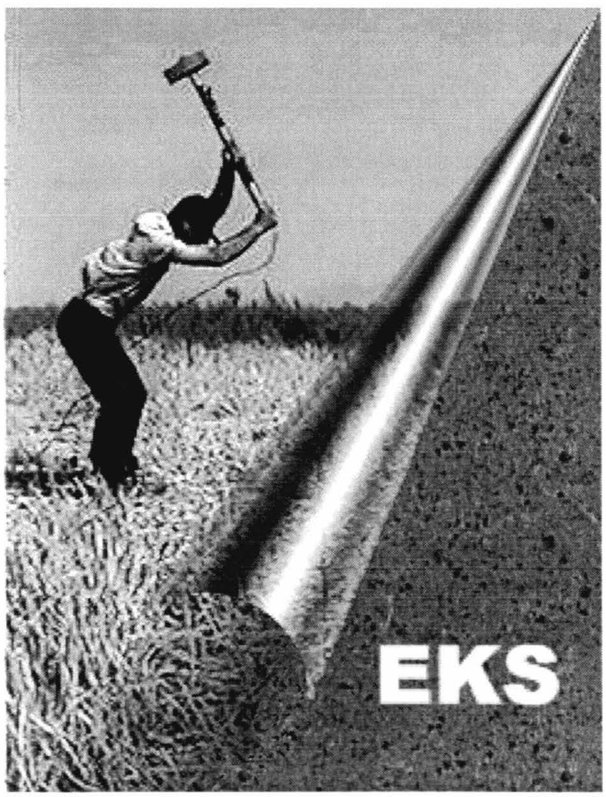

Bibliographic Reference :
Beamish D., 1998.
Electrokinetic Sounding Results, INCO-DC Project 950176, Cyprus, 1997.
British Geological Survey, Technical Report, WE/98/23

A report prepared for:
European Commission
DG-XII
Directorate B
Programme INCO-DC
75, Rue Montoyer
B-1040 Brussels

British Geological Survey, Keyworth, Nottingham, 1998

CONTENTS

1) Introduction

This report summarises the results of work undertaken for the EEC INCO-DC project: A new integrated geophysical approach for the rational management and exploration of groundwater resources. The programme Project Number is 950176 under Contract Number ERBIC 18 CT 960122.

EU member participants are:

The Netherlands:	RGD: (NITG-TNO), Haarlem James Baker (Project Coordinator)
France:	BRGM, Orleans Alain Beauce
U.K.:	BGS, Nottingham D. Beamish and Jon Busby

Non-EU partners are:

Cyprus:	GSD, Nicosia Sortiris Kramvis	GEOINVEST, Nicosia Andreas Shiathas
Israel:	GII, Holon Mark Goldman	

A previous report summarised the field activities of the Electrokinetic Sounding (EKS) technique which took place on Cyprus during June 1997 (Beamish, 1997). Geophysical surveys on Cyprus are designated as Task 3 and the EKS technique designated as sub-task 3.5. EKS fieldwork took place in the Astromeritis-Kokkinotrimithia area of the western Mesaoria. The geology/hydrogeology of the project area on Cyprus has been summarised in an unpublished project document by GSD.

2) Cyprus Field Work

EKS data collection took place between June 03 and June 13 1997 and data were collected along three main profiles designated :

1) Potami
2) Astromeritis
3) Meniko

Profile coordinates of the EK soundings and other information are given in Table 1. The previous report shows the sounding coordinates in map form of the three profiles. Other geophysical surveys conducted along the profiles during 1997 included PMR (BRGM), TDEM (GII), AMT (BRGM) and VLF (GSD). The geophysical techniques are Proton Magnetic Resonance (PMR), Time Domain Electromagnetic Sounding (TDEM), Audiomagnetotelluric sounding (AMT) and Very Low Frequency electromagnetics (VLF).

A single day was used acquiring test data on the Troodos Pillow Lavas (northern fringe of the Troodos Ophiolite) in the Klirou area. A detailed profile of measurements (5 m intervals) was obtained across the location of an Azimuthal Resistivity Sounding (BGS).

Thirteen main EK soundings were obtained along the predominantly NW-SE Potami profile (Table 1). Site codes are sequential from the first sounding (01, at a profile distance of 200 m) through to 13 (profile distance of 1800 m). Twelve main soundings were obtained along the predominantly E-W Astromeritis profile. Site codes are sequential from the first sounding (14, at a profile distance of 70 m) through to 25 (profile distance of 1640 m). Nine main soundings were completed along the NW-SE Meniko profile. Site numbers (0 to 1210) refer to distance along the profile.

EK data were not acquired in a routine manner since the technique remains experimental. Figure 2.1 summarises some of the dipole array configurations used. A large number of sub-experiments were needed to attempt to improve the methodological procedures for the survey conditions in the western Mesaoria. This requirement was particularly acute due to the very low EK signal amplitudes experienced. Dipole voltages were a factor of 10 below levels associated with typical sandstone environments.

The previous report (Beamish, 1997) discusses survey data acquisition using the BGS EKS system. This report considers the EK data collected during the survey and the results obtained. Since the technique is susceptible to a number of noise sources these are discussed first with particular reference to the Klirou area data. The quality of a final (stacked) EK sounding is determined by the stacking procedure and the degree of the residual noise components following stacking. These are discussed using examples from various survey locations. The following two sections offer a brief summary of some of the subsidiary experiments (acoustic and EK profiling) that were carried out at various stages of the survey. These are followed by a section summarising the main sounding results for each of the three survey profiles. The final section of the report provides the conclusions of the study.

3) Noise Sources

3.1) Typical noise

The procedure of data (shot) stacking is illustrated in Figure 3.1 using data from the Astromeritis profile (sounding E1210). Ten successive shot records from channels 1&2 are superimposed (thin lines) with the 10-shot stack average shown as a heavier line. The larger amplitude EK coupling voltage occurs within the first 20 ms with a maximum excursion of < 0.20 mV/m. At later times the ten shot records display a variety of noise sources with the resulting stack average displaying incomplete (i.e. non-zero) out-of-phase residuals. The amplitude of the residuals can be governed by a small number of records with larger (than average) noise components.

The purpose of EK data processing is to minimise the records with specific noise sources that may degrade the stacking procedure. When the signal levels are low (e.g. less than 0.5 mV/m) then the problem of EK signal detection at late times becomes particularly difficult. One source of noise are sferics as shown in Figure 3.2. Large amplitude sferics can exceed 1 mV/m and can be much larger than EK signal amplitudes. Large amplitude sferics are relatively rare and occur as a burst over several milliseconds.

More typical persistent higher frequency noise is illustrated in Figures 3.3 and 3.4 using records from the Potami profile. In these figures successive records of 10 ms duration are shown for the record interval 100 to 110 ms. All are plotted to a common scale as shown by the scale bar. Figure 3.3 shows data from sounding E09 on channels 3&4 (2m dipoles, centres at +/- 2.5 m).At the scale shown there is no evidence for repeatable in-phase behaviour. The same data recorded on channels 5&6 (2m dipoles, centres at +/- 3 m, Fig. 3.4) is much smaller in amplitude but similar noise characteristics are observed.

Different forms of noise behaviour at a further two sites on the Potami profile (E10 and E11) are shown in Figures 3.5 and 3.6. The superimposed spectra (FFT) of 16 shot records are shown in Figure 3.7 (a,b). In the 3.7a, the data is unprocessed (i.e. unfiltered) and a peak at 50 Hz is observed but the major frequency components occur at about 200 Hz and at higher frequencies. The result of 50 Hz mains removal and low-pass filtering the data are shown in Figure 3.7b. Although the 50 Hz component can be suppressed, the records remain dominated by high frequency noise components.

3.2) Noise Sources - Klirou

A single day was used acquiring test data on the Troodos Pillow Lavas (northern fringe of the Troodos Ophiolite) in the Klirou area. A detailed profile of measurements (5 m intervals) was obtained across the location of an Azimuthal Resistivity Sounding. The data quality obtained along the 100 m profile was poor and many soundings displayed a variety of:

large amplitude noise
inconsistent (time-dependent) behaviour.

In many cases the electrodes had to be hammered into hard rock. Electrode contact resistances were monitored and remained low (e.g. 1.5 kohm.). Some effects observed may be due to 'plate-bounce'. Figure 3.8 shows 10 repeat shots of the two inner channels at profile location 25 m. Apart from the first EK pulse (0 to 20 ms) noise sources are large producing a poor quality stack (thick lines). Similar poor quality sounding behaviour is observed at profile location 50 m (Figure 3.9) although here the degree of high frequency noise is less severe. A highly complex set of shot records from profile location 75 m is shown in Figure 3.10. Large out-of-phase pulses can be seen at times > 80 ms. These are shown more clearly over the time-interval from 60 to 240 ms in Figure 3.11. The source of this noise is unknown (plate bounce?). Overall the EK data quality obtained in the Klirou area was the lowest obtained during the survey.

3.3) Background noise tests

Background noise tests were carried out at location 1322 m on the Meniko profile. The location is some 112 m beyond the final sounding (1210 m) of the Meniko profile. High frequency (i.e. in the kHz range) noise contributions appeared to increase with increasing distance along the Meniko profile. The examples shown here represent the most severe noise contamination experienced during the survey. For the tests dipole lengths were 10 m, the sampling rate was reduced to 5 kHz and gains were set to unity. Channel 1 is along the profile direction and channel 2 is perpendicular to the profile direction.

Figure 3.12 shows 400 ms of background data from the test with a scale bar indicating amplitude. The two pairs of traces (1&2 and 3&4) represent orthogonal pairs of dipoles. The predominant lower frequency 'continuous' oscillation on channels 1 and 3 (along profile) is 100 Hz. A much larger amplitude (towards 1 mV/m) burst-mode, higher frequency oscillation occurs in the orthogonal direction (trace numbers 2 and 4). This behaviour is repeated throughout the test data as shown in Figure 3.13.

Spectra from 10 successive shot recordings are overlaid in Figures 3.14 (conventional FFT) and 3.15 (maximum entropy). The results confirm the absence of 50 Hz (and mains harmonic) components and the strength of the 100 Hz and higher frequency (>500 Hz) noise components. The occurrence of the 100 Hz oscillation is particularly unfortunate as the majority of noise reduction procedures are concerned with 50 Hz and odd-harmonic components.

4) Stacking Residuals

Following the production of final stacks for each sounding, the data are examined for in-phase behaviour across each pair of shot-symmetric dipoles and across the array of dipoles. Figure 4.1a shows 'typical' early time behaviour from a linear (in-line) sounding (E05 from the Potami profile). Usually the traces are examined in 'trace-normalised' form as shown. In this example, channels 1 to 3 are obtained from symmetrical, 2-m dipoles (centres at +/- 1.5, 2.5 and 3 m). Channel 4 is a 4-m dipole between +/- 1 to 4 m. the example shows:

> An 'arrival time' difference between channels 1 and 4, and subsequent moveout at an apparent velocity of about 125 m/s.
> An apparent change in character between channels 1 and 2&3.
> Moveout over the 1 m distance separating channels 2 and 3.

When examining trace-normalised data, the rapid decay of EK amplitudes away from the shot point should be noted. Figure 4.1b shows the same data as Figure 4.1a but in true amplitude (scale bar of 0.2 mV/m). This type of behaviour was repeated throughout the survey.

The 40 ms time interval from 100 to 140 ms, for the same sounding is shown in true amplitude form in Figure 4.2. Peak-to-peak amplitudes are < 5 microvolts and in some portions of the record (e.g. 130 to 140 ms), oscillations are coherent across the array. These are noise-residuals caused by incomplete cancellation (of the stacking procedure) at the microvolt level. It should be noted that the noise sources are 'phase-locked' between records since the 8 channels are acquired simultaneously. A further example of noise-residuals from the same sounding (200 to 240 ms) is shown in Figure 4.3. At these later times, the residual noise level has reduced to < 2 microvolts peak-to-peak.

The form (amplitude and time-persistence) of noise can vary from site to site. Figure 4.4 shows a true amplitude display from the linear in-line sounding E11 (1600 m along the Potami profile) for the 40 ms interval from 100 to 140 ms. These data display small residuals (a few microvolts) that show a high out-of-phase correlation between symmetric dipole pairs and a high correlation across the dipole array.

The character of the noise residuals from an azimuthal sounding is shown in Figure 4.5. These data are from sounding E24 at 1490 m along the Astromeritis profile. The true amplitude plot shows that between 100 and 140 ms, typical residual amplitudes are at the microvolt level and are coherent across the two in-line combinations of dipoles (i.e. channels 1&2 and 3&4).

5) Acoustic Data

Small scale refraction experiments were carried out at a few selected locations as indicated in Table 1. Generally, offset distances extended to only 8 m and, consequently, the velocity information obtained was confined to very shallow depths in the vicinity of the source.

Figure 5.1 shows the acoustic data recorded at sounding 01 (200 m) on the Potami profile. These data are typical of the acoustic data recorded during the survey. Data from the first four channels (offsets to +/- 2 m) suffer saturation during the first 50 ms. First break (direct arrival) velocities are estimated at 1032 m/s with subsequent arrivals over the first 40 ms having slower apparent velocities of 545 m/s.

Typical maximum entropy power spectra for the data obtained at offsets between 1 and 8 m are shown in Figures 5.2a and 5.2b. In Figure 5.2a, the first 2000 data points (0-200 ms) of the recording are analysed. The major acoustic energy components occur between 50 and 70 Hz. In Figure 5.2b, the second 2000 data points (200 to 400 ms) of the recording are analysed. In this section of the record, the major acoustic energy components are less dispersed and again occur between 50 and 70 Hz with a secondary peak at around 200 Hz.

6) EK Profile Data

At a number of locations, detailed (5m) profiles were obtained in the vicinity of the major soundings (see Table 1). The detailed experiments involved just two symmetric 2 m dipoles (0.5 to 2.5 m) and used a reduced number of shots (20 to 40) to maintain a reasonable acquisition rate.

Figures 6.1a and 6.1b show the data that were obtained in the vicinity of sounding EP08 (1210 m, Potami profile). Figure 6.1a displays the first 40 ms of trace normalised data along the profile from 5 to 95 m for channel 1. It should be noted that voltage amplitudes are low and the trace normalisation will amplify noise as well as signal. Certain features within the first 30 ms display a degree of lateral persistence across the whole profile (e.g. a negative, to the left, excursion between 10 and 14 ms). Most features however show a poor persistence across the profile. The general behaviour is repeated for the shot-symmetric channel 2 data shown in Figure 6.1b.

7) Summary of Data Characteristics

In order to summarise the data characteristics, only the behaviour of the first two channels (invariably the most sensitive) obtained from two metre dipoles (+/- 0.5 to 2.5 m) are used. The use of only the first two (inner) channels may not totally represent the sounding characteristics at a particular site. Figure 7.1 shows the trace-normalised behaviour of four symmetrical channels (sounding EP19, 780 m, Astromeritis profile). Two metre dipoles are used for the first 3 pairs (centres at +/- 1m, 2m and 3 m). The fourth pair (shown as channel 4) uses a 4 m dipole between +/- 0.25 and 4.25 m). As shown in Figure 5.1, the two channel 3 traces (+/- 3 m) display a much higher level of 'in-phase' behaviour than the other pairs of channels.

Soundings from the three profiles are considered in sequence. The data are divided into two time segments each of 40 ms in duration (0-40, 40-80) followed by two time segments each of 80 ms duration (80-160 and 160 to 240 ms). All the data are shown trace normalised.

7.1) Potami profile

The first seven soundings (01 to 07, covering profile distances from 200 to 1100 m) are shown in Figures 7.2a to 7.2d. In the first time segment (0-40 ms) only soundings 5 and 7 display good EK signal. In the second time segment (40-80 ms) only sounding 7 retains in-phase behaviour. The data through the second two time segments (80-160 and 160-240 ms) display noise behaviour.

The second seven soundings (07 to 13, covering profile distances from 1100 to 1800) are shown in Figures 7.3a to 7.3d. In the first time segment only soundings 7 (repeated), 8 and 10 display good levels of EK signal. In the second time segment only sounding 7 retains in-phase behaviour. The data through the third time segment begin to display high frequency in-phase behaviour at sounding 11. By the fourth time segment various forms of high frequency in-phase behaviour can be observed at soundings 10, 11 and 12.

7.2) Astromeritis profile

The first six soundings (14 to 19, covering profile distances from 70 to 780 m) are shown in Figures 7.4a to 7.4d. No EK signal is apparent at any of the sites over the time interval shown (0 to 240 ms).

The second six soundings (20 to 25, covering profile distances from 960 to 1640 m) are shown in Figures 7.5a to 7.5d. Again there is no evidence of good EK coupling over the time intervals displayed. At sounding 22 (number 3 in Figures 7.5) a high frequency, in-phase oscillation begins during the interval 40-80 ms. With the gradual decay of low frequency oscillations at later times, the in-phase behaviour becomes more evident.

7.3) Meniko profile

The eight soundings obtained along the Meniko profile (0 to 1210 m) are shown in Figures 7.6a to 7.6d. With the possible exception of sounding 1110 m (number 7 in Figures 7.6) there is no evidence of in-phase EK behaviour at any of the soundings along the Meniko profile. None of the data obtained along the Meniko profile showed high-frequency, in-phase behaviour.

8) Summary and Conclusions

The Electrokinetic technique is experimental and research intensive. This report has presented only a small portion of the data that were collected during the survey. The survey data, obtained along three profiles in the western Mesaoria, were all characterised by low amplitudes with early-time (0-20 ms) voltage excursions confined to the sub-millivolt range. These are a factor of ten below signal amplitudes typical of sandstone environments.

It was also found that the signals were spatially compact and large offset (i.e. > 5 m from the shot point) recording was not appropriate for the environment. Co-linear recording arrays were replaced by azimuthal configurations which maintained dipole offsets close to the shot point.

The low amplitude signal levels experienced meant that the detection of later-time (deep) sources of EK coupling was particularly problematic. The report has discussed the noise sources that were encountered. Power line sources (50 Hz and odd harmonics) were not excessive and the processing algorithms dealt with these efficiently. The most severe electromagnetic noise contamination occurred with increasing distance along the Meniko profile. Here a strong 100 Hz noise component was detected together with bursts of higher frequency (> 500 Hz) noise components. It is stressed that it is the poor environment for EK coupling, rather than noise sources, that has led to the lack of any detectable signal from deep interfaces.
Detailed examinations of the final stacked data have revealed that EK signal, where detected, is largely confined to the first 40 ms of the record. The only sounding to exhibit later-time coupling was 07 (1100 m) of the Potami profile. All the coupling effects observed display moveout behaviour and are therefore associated with horizontally-propagating wave components. No simultaneous EK coupling effects were detected.

In summary, EK coupling effects observed during the survey were low amplitude effects arising from near-surface, shallow interfaces. The low amplitudes associated with the marl/mudstone environment of the western Mesaoria provided data that mitigated against the detection of late-time coupling from deeper interfaces. The data could not resolve any effects associated with the deep target aquifers. It is also noteworthy that the PMR survey conducted by BRGM over the same profiles, found a 'no signal' region within the western Mesaoria. The cause of the effect is under investigation.

9) References

Beamish, D., 1997. Summary of field activities: Year 1, INCO-DC Project 950176, Electrokinetic Sounding. British Geological Survey Technical Report, WE/97/44.

10) Acknowledgements

It is a pleasure to acknowledge the major contribution made by the GSD, Nicosia during the field work. Many members of staff were involved and I thank Sortiris Kramvis for his organisational skill together with his reassuring ability to solve problems as they arose.

Table 1 **Cyprus-97**

Electrokinetic Soundings Coordinates

3 Main profiles

POTAMI

	East (m)	North (m)	Distance (m	Type
01+	503.715	885.070	200	Linear
02	503.645	885.259	500	Linear
03+	503.540	885.500	700	Linear
04	503.490	885.593	800	Linear
05	503.448	885.696	900	Linear
06	503.386	885.775	1000	Linear
07	503.319	885.858	1100	Linear
08P	503.279	885.945	1200	Linear
09	503.220	886.055	1295	Linear
10	503.180	886.120	1560	Linear
11	503.080	886.300	1600	Linear
12	503.032	886.389	1700	Linear
13	502.986	886.480	1800	Linear

ASTROMERITIS

	East (m)	North (m)	Distance (m	Type
14	504.140	889.775	70	Linear
15	504.250	889.795	180	Linear
16+	504.380	889.843	325	Linear
17+	504.515	889.838	480	Linear
18+	504.650	889.868	620	Linear
19P	504.813	889.870	780	Linear
20	505.005	889.898	960	Linear
21	505.112	889.905	1070	Linear
22+P	505.220	890.035	1216	Azimuthal
23	505.403	889.990	1396	Azimuthal
24	505.475	890.045	1490	Azimuthal
25	505.628	890.042	1640	Linear

MENIKO

	East (m)	North (m)	Distance (m	Type
0	514.957	883.425	0	Azimuthal
162	515.094	883.266	162	Azimuthal
312	515.200	883.165	312	Azimuthal
600	515.405	882.952	600	Azimuthal
814	515.546	882.800	814	Azimuthal
909	515.620	882.713	909	Azimuthal
1000	515.670	882.644	1000	Azimuthal
1110	515.748	882.566	1110	Azimuthal
1210	515.827	882.485	1210	Azimuthal

Site codes ending in + have acoustic data

Site codes ending in P have local EK profiles

Figure 2.1. Summary of electrode configurations. All arrays are slit-spread and symmetric about the shot-point. Dipole length is 2 m.

a) 2-channel. All arrays contain 'inner' 2 dipoles
b) 4-channel azimuthal array
c) 10-channel, contiguous array.
d) 16-channel, overlapping array.

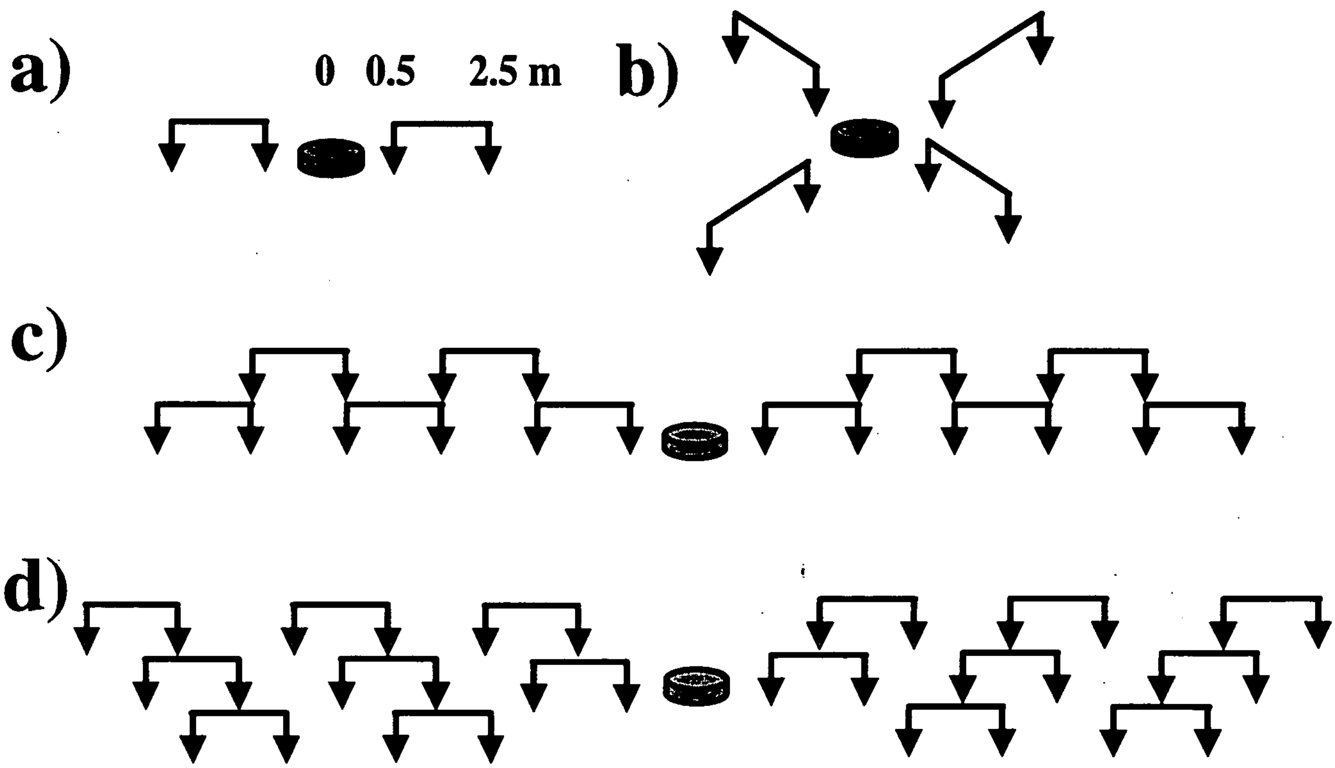

Figure 3.1 Example of data repeatability. Ten shots showing data from two shot-symmetric dipoles overlaid.

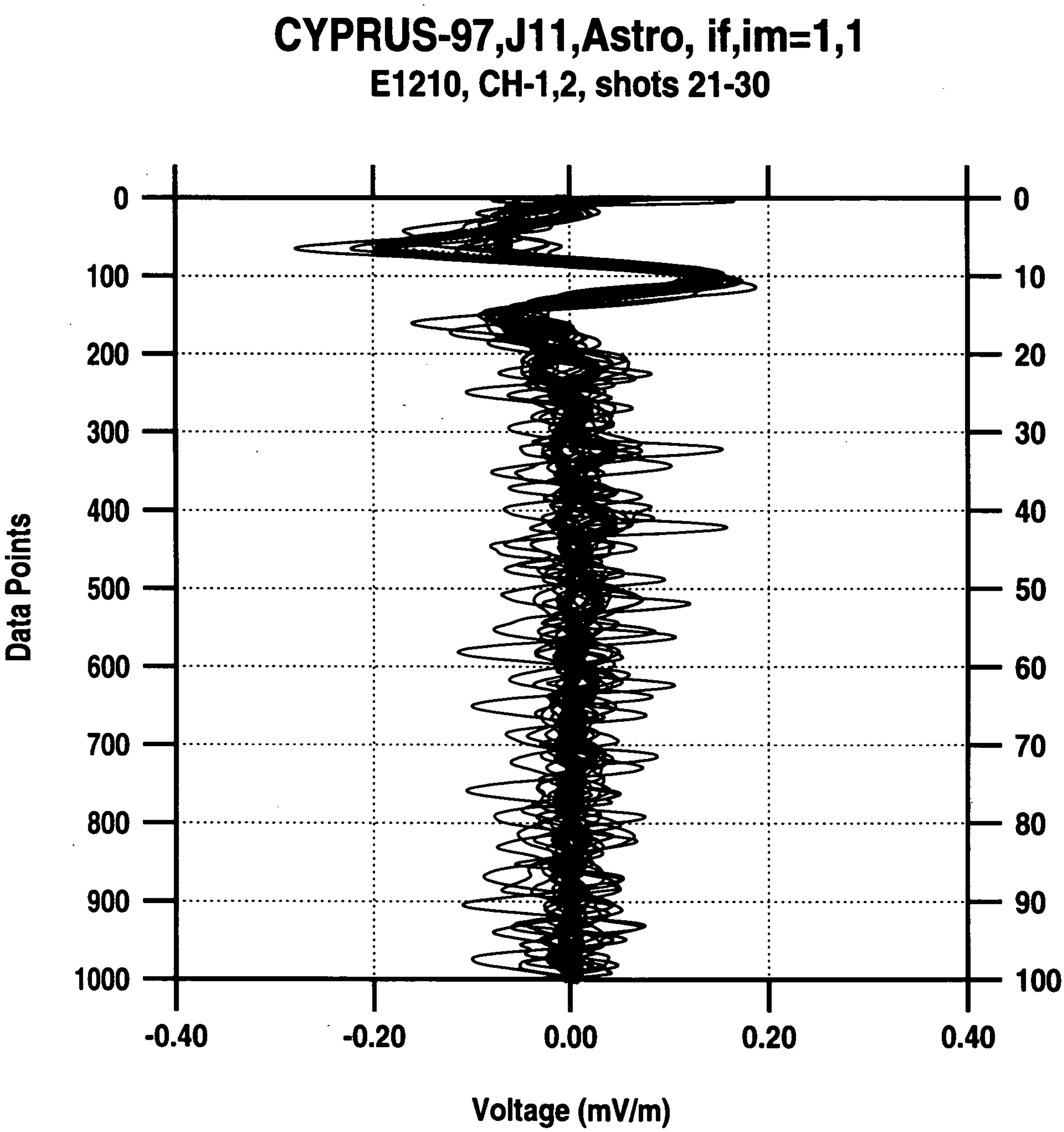

Figure 3.2 Example of a noise source. Sferic recorded in two symmetric channels lasting about 5 ms.

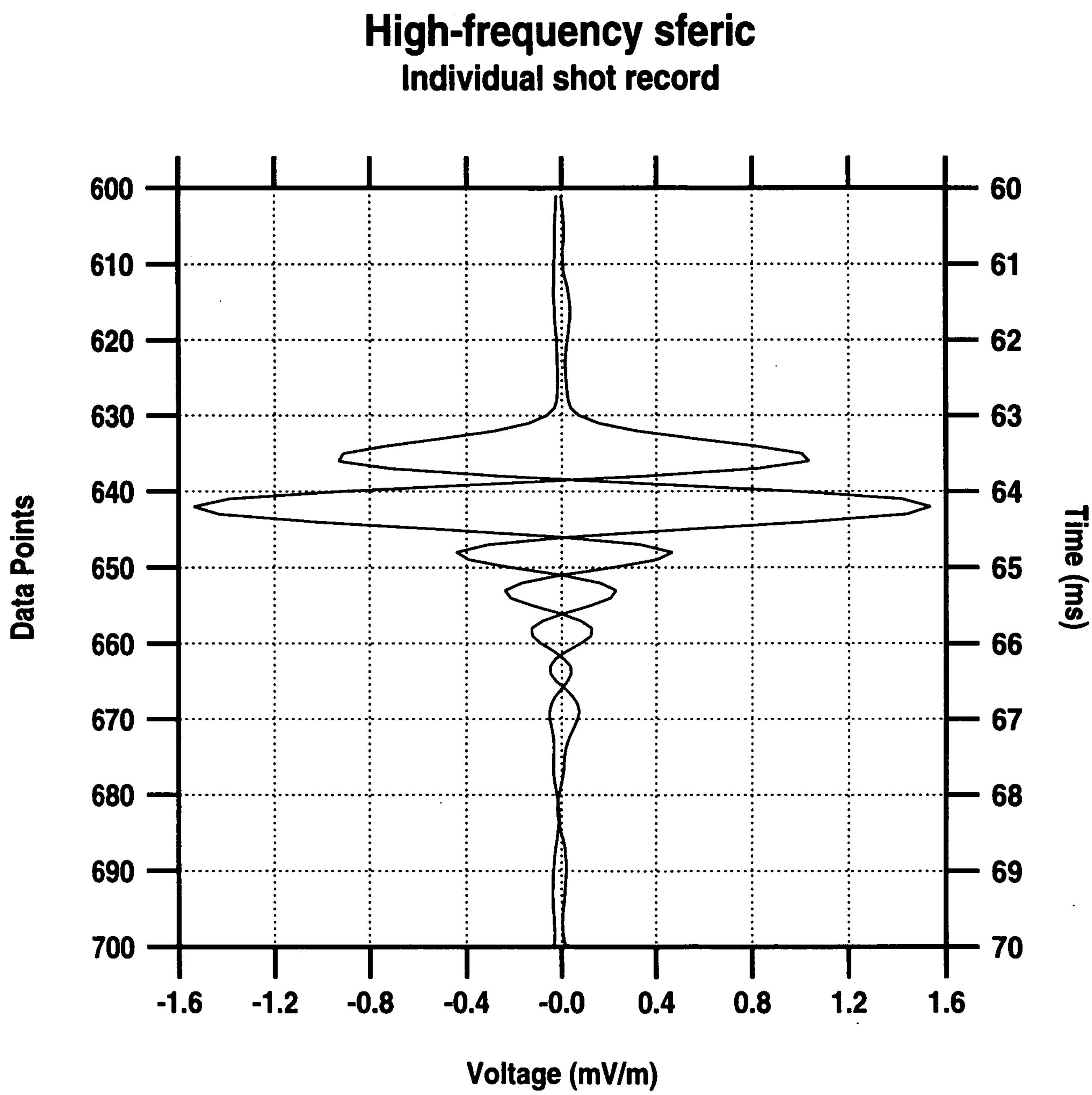

Figure 3.3 Examples of successive shots records from 2 shot-symmetric channels (overlaid) for each shot number. Sounding E09. Channels 3&4. Scale bar shows amplitude.

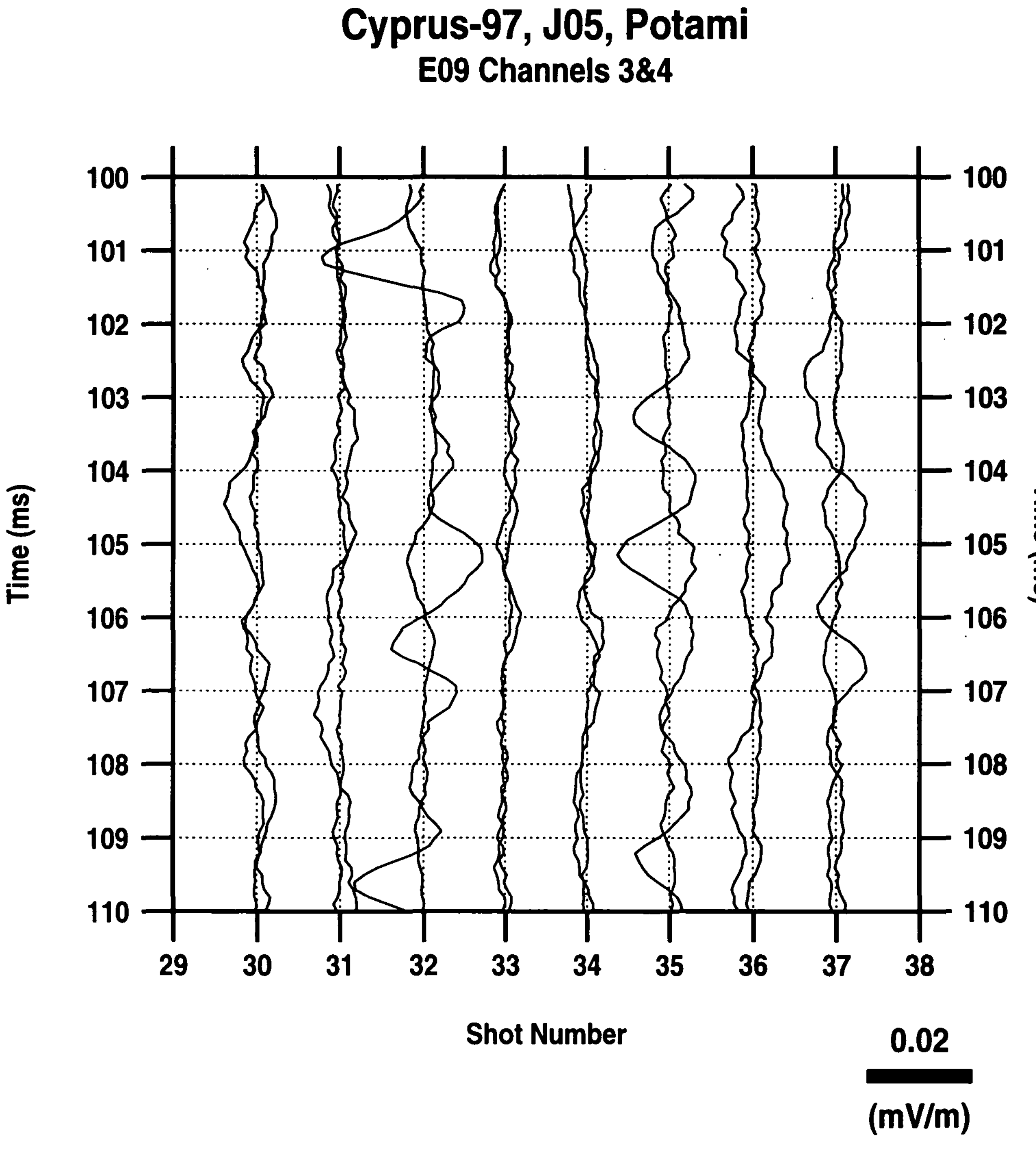

Figure 3.4 Examples of successive shots records from 2 shot-symmetric channels (overlaid) for each shot number. Sounding E09. Channels 5&6. Scale bar shows amplitude.

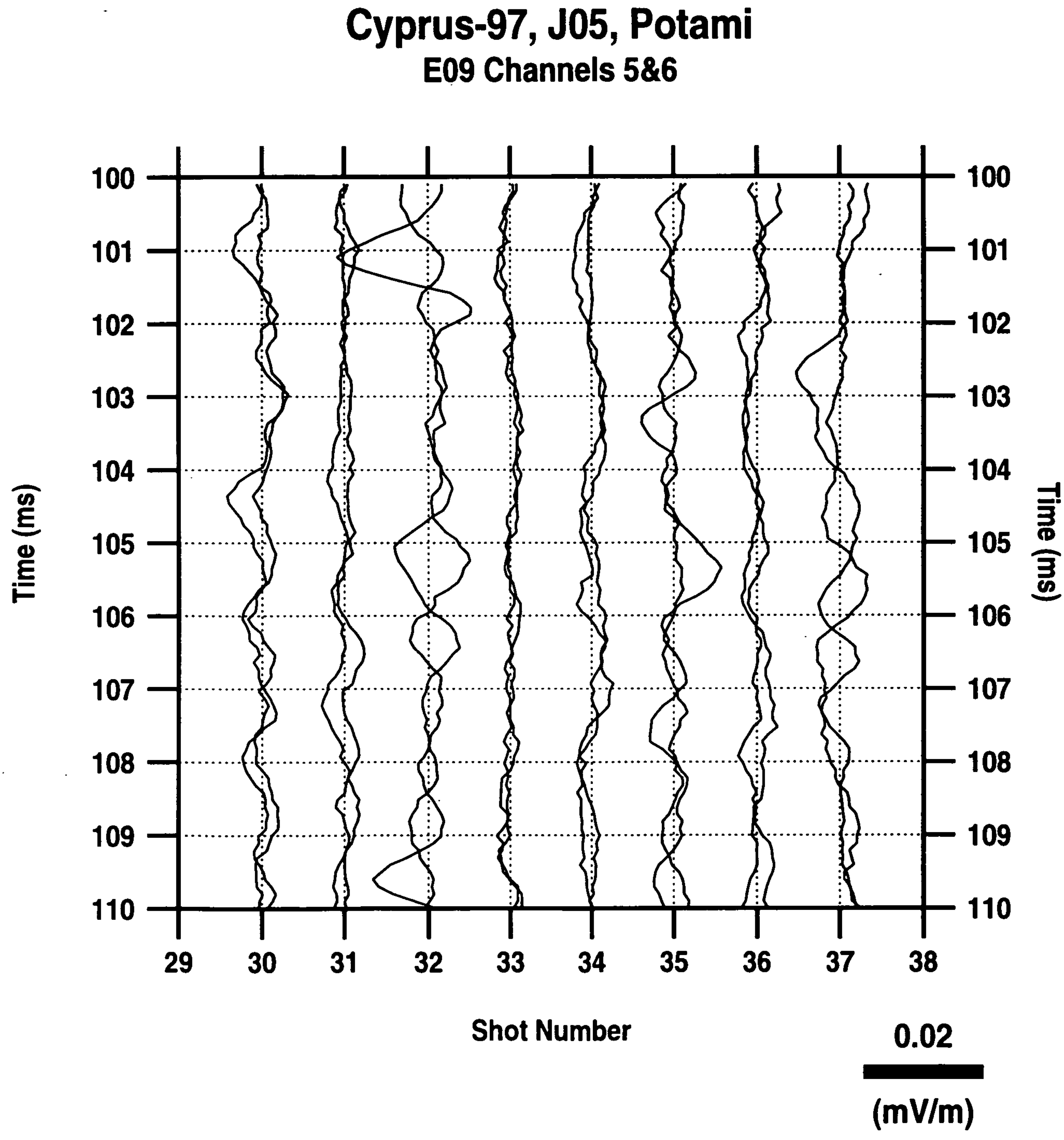

Figure 3.5 Examples of successive shots records from 2 shot-symmetric channels (overlaid) for each shot number. Sounding E10. Channels 5&6. Scale bar shows amplitude.

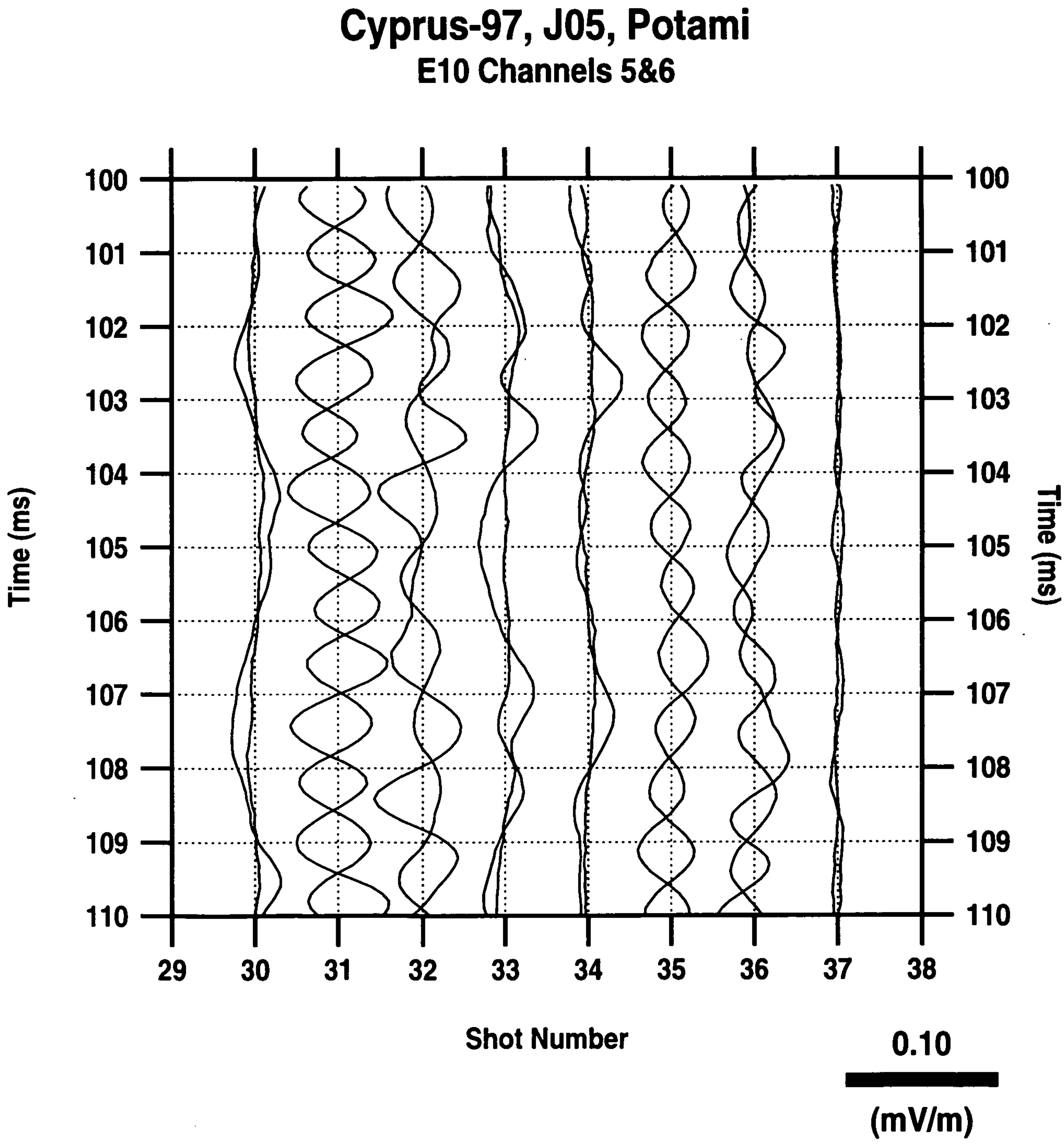

Figure 3.6 Examples of successive shots records from 2 shot-symmetric channels (overlaid) for each shot number. Sounding E11. Channels 5&6. Scale bar shows amplitude.

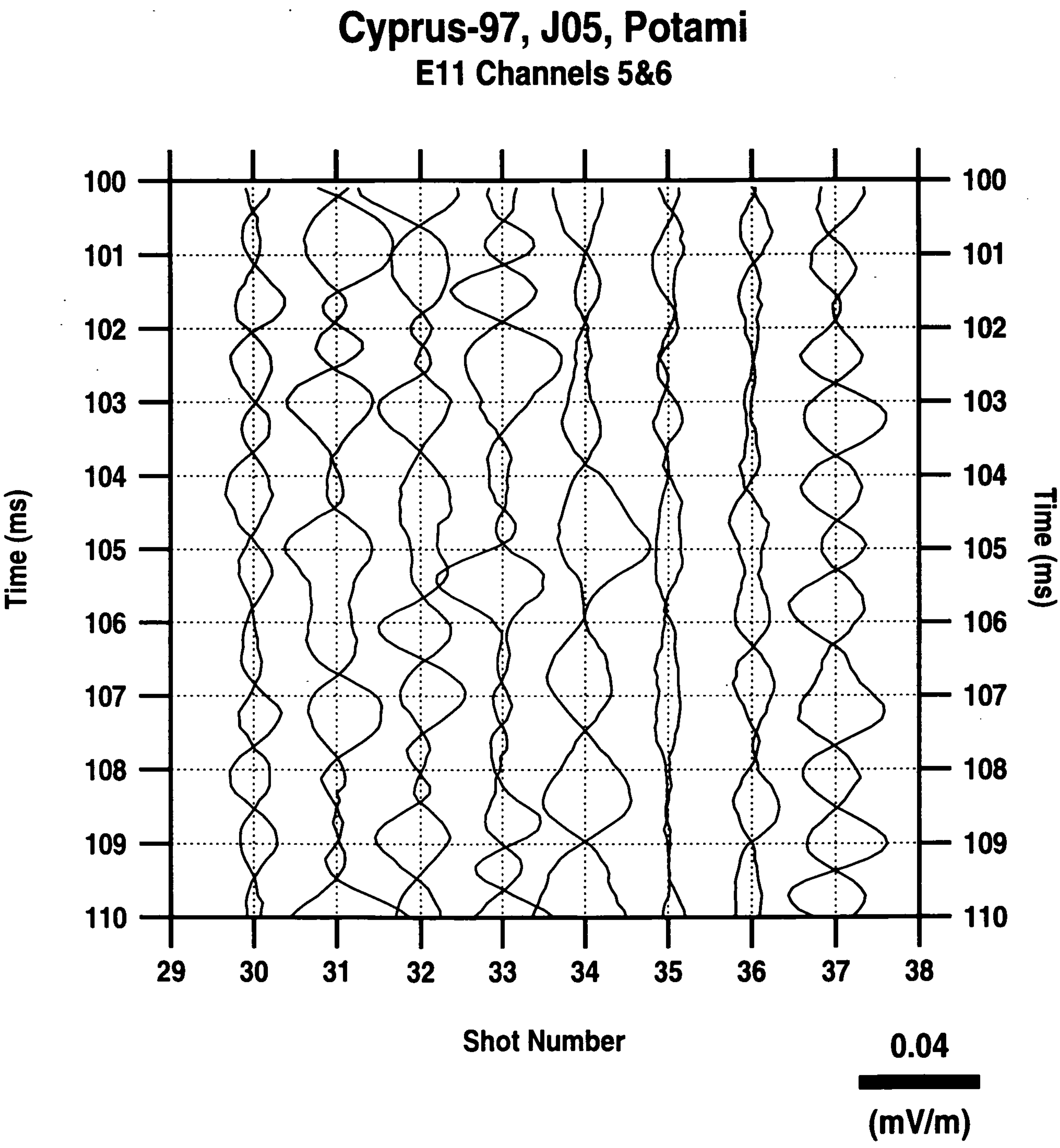

Figure 3.7a Example of frequency spectra from successive shots (overlaid). No mains (50 Hz) filtering. Sounding E10. Channel 5.

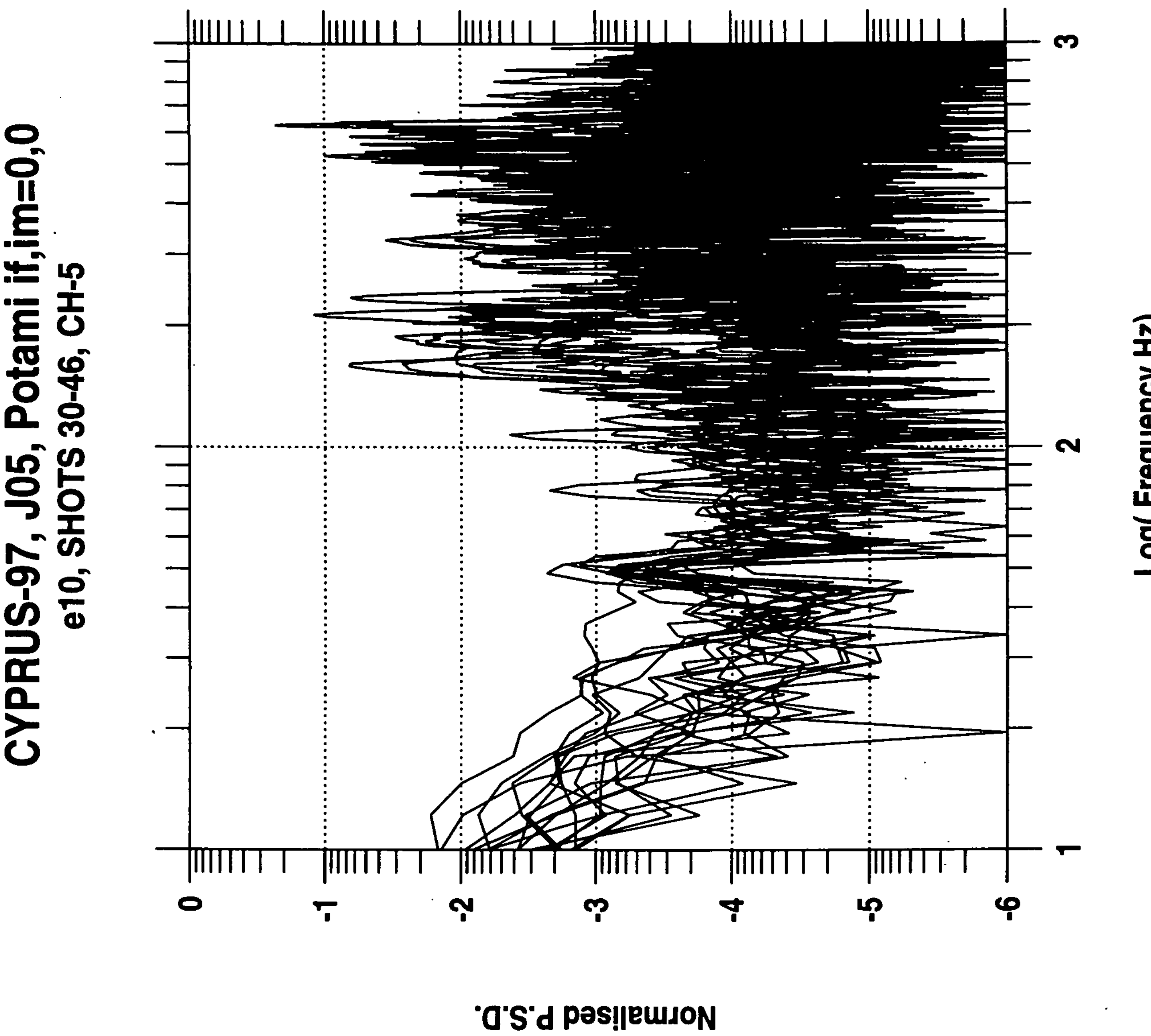

Figure 3.7b Example of frequency spectra from successive shots (overlaid). Mains (50 Hz) filtering applied. Sounding E10. Channel 5.

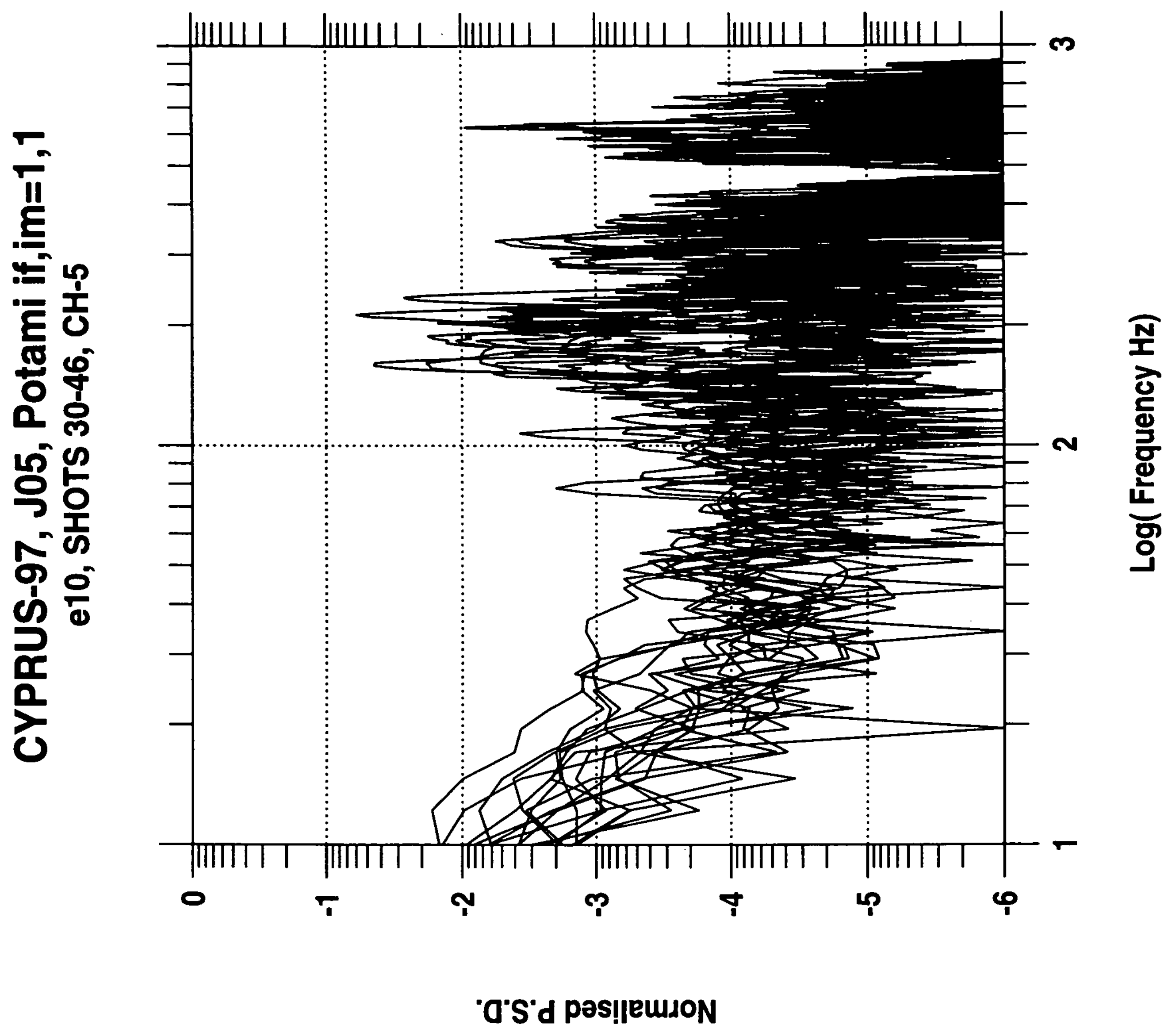

Figure 3.8 Example of data repeatability from Klirou survey. Ten shots showing data from two shot-symmetric dipoles overlaid. Sounding at 25 m along profile.

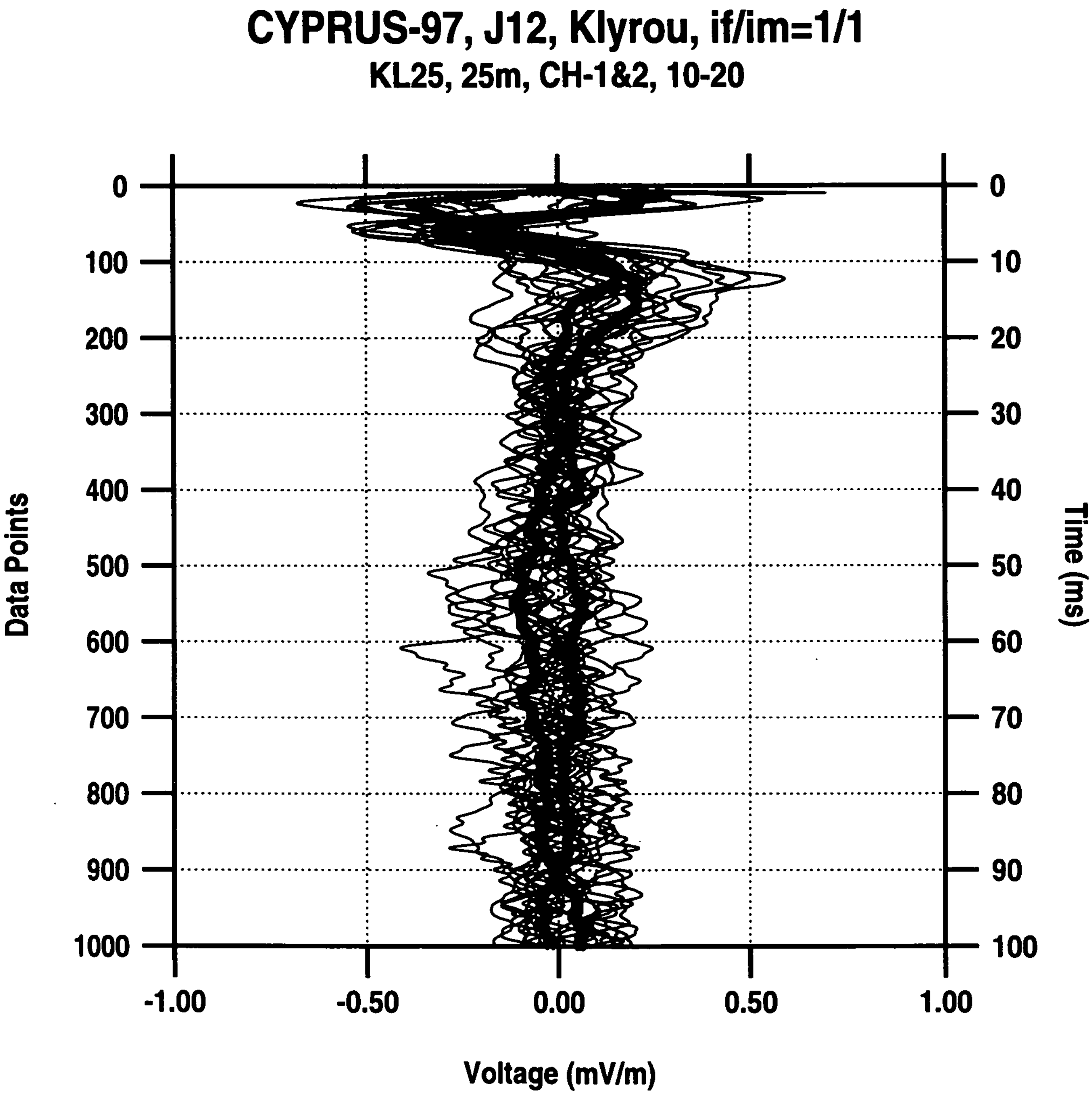

Figure 3.9 Example of data repeatability from Klirou survey. Ten shots showing data from two shot-symmetric dipoles overlaid. Sounding at 50 m along profile.

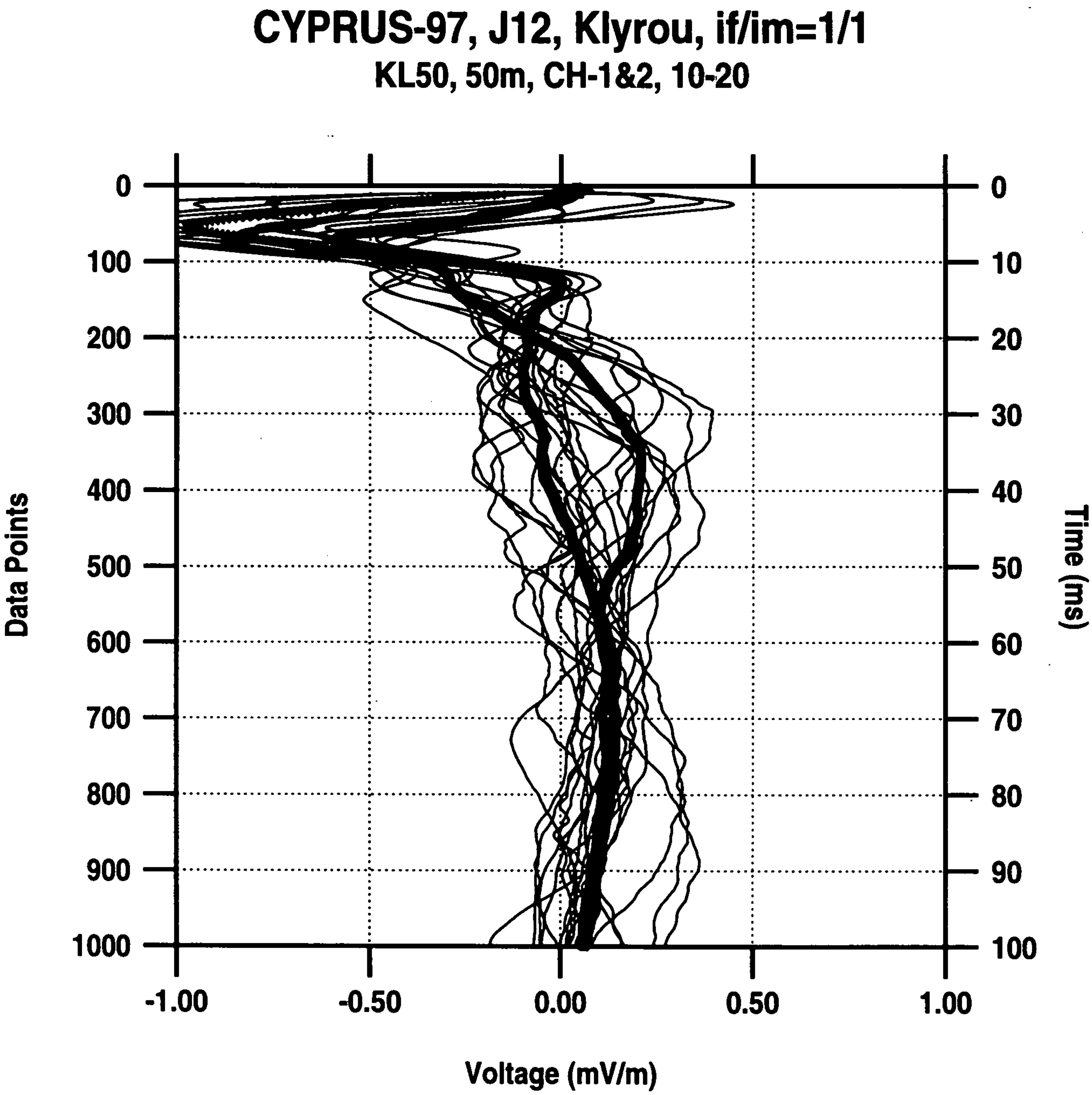

Figure 3.10 Example of data repeatability from Klirou survey. Ten shots showing data from two shot-symmetric dipoles overlaid. Sounding at 75 m along profile.

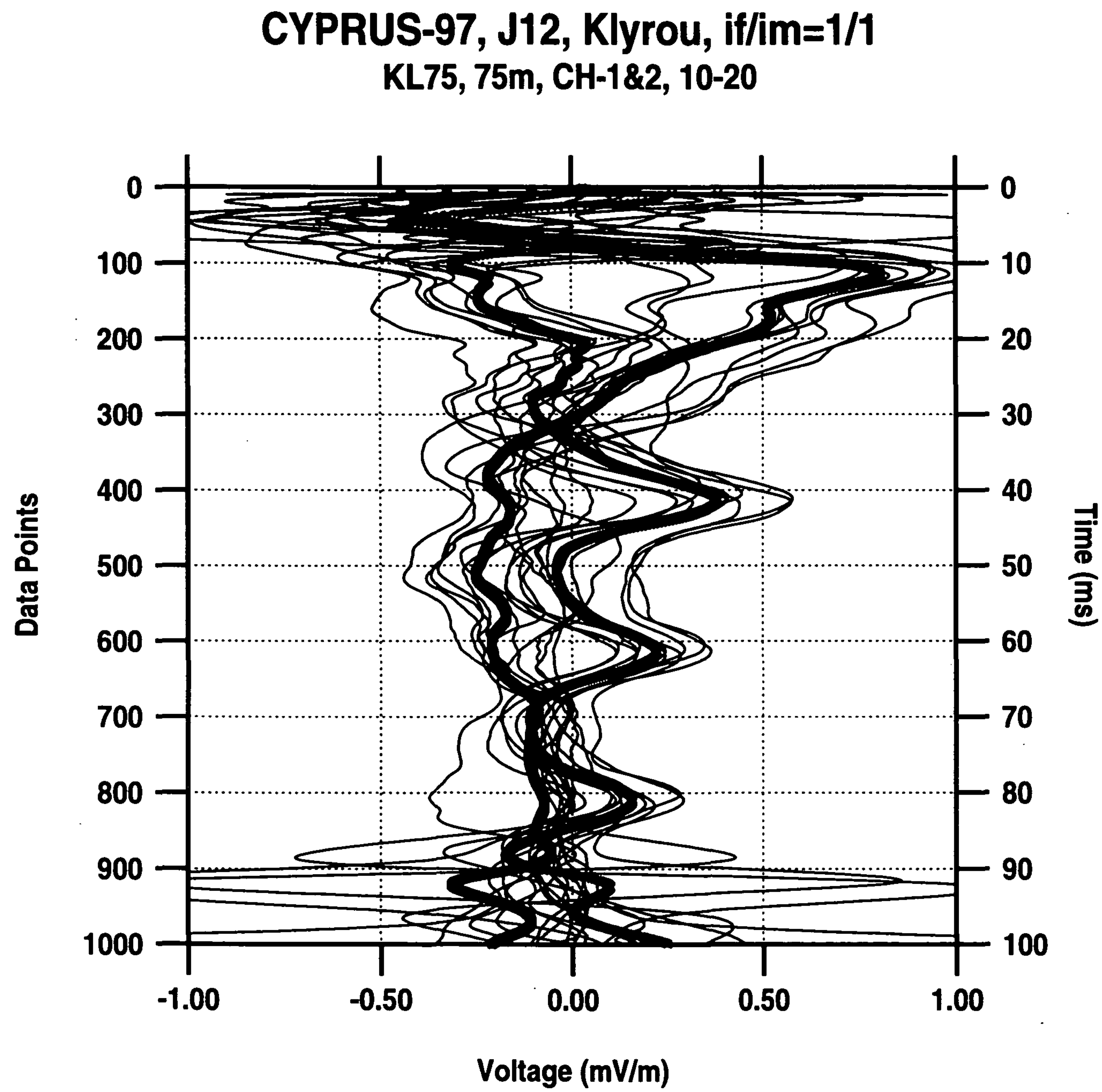

Figure 3.11 Example of data repeatability from Klirou survey. Ten shots showing data from two shot-symmetric dipoles overlaid. Sounding at 75 m along profile. Time interval 60 to 240 ms.

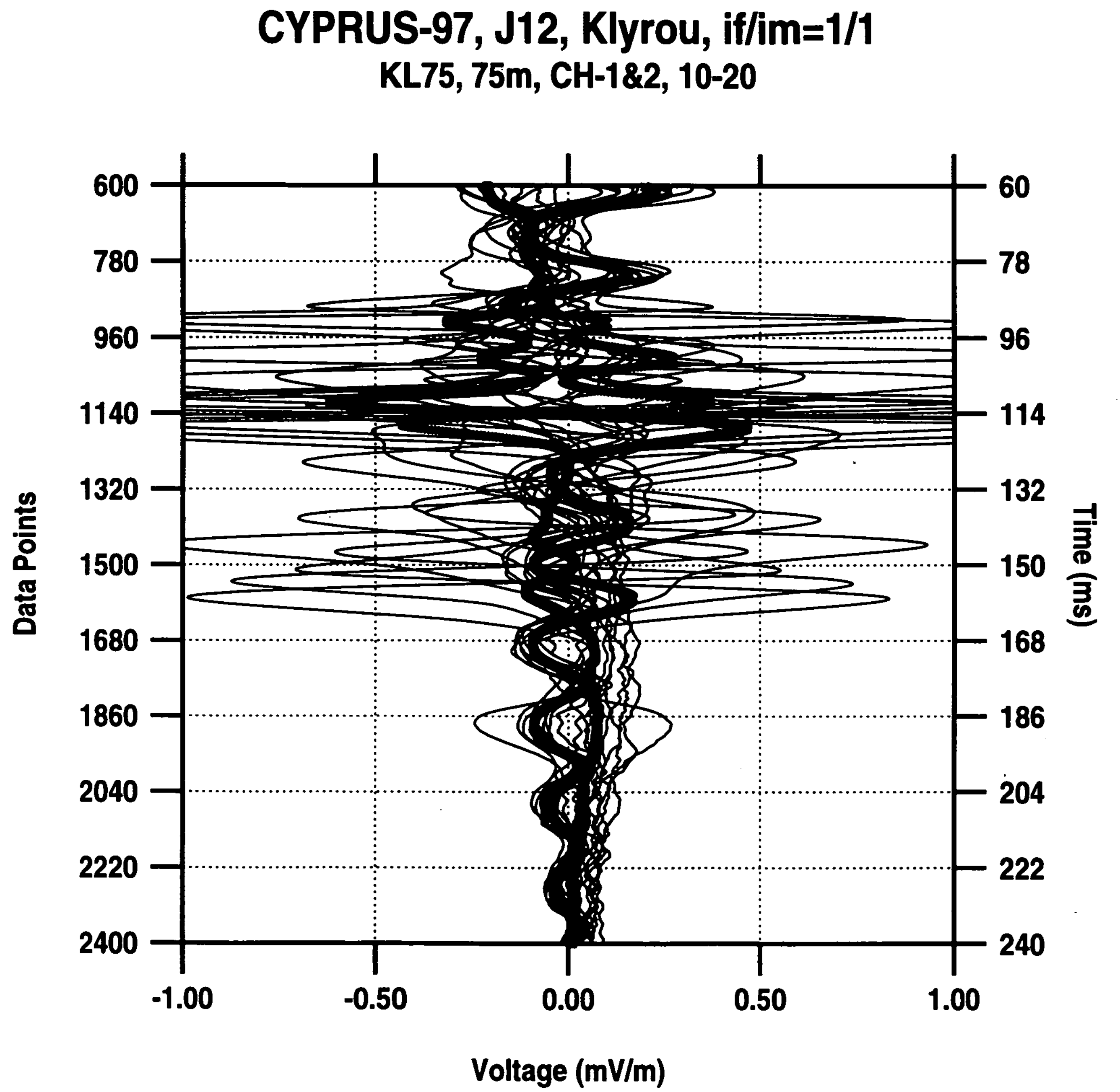

Figure 3.12 Example of high frequency noise sources - Meniko profile. Background noise tests (no acoustic source) using 10 m orthogonal dipoles. One record (orthogonal channels 1&2), next record (orthogonal channels 3&4).

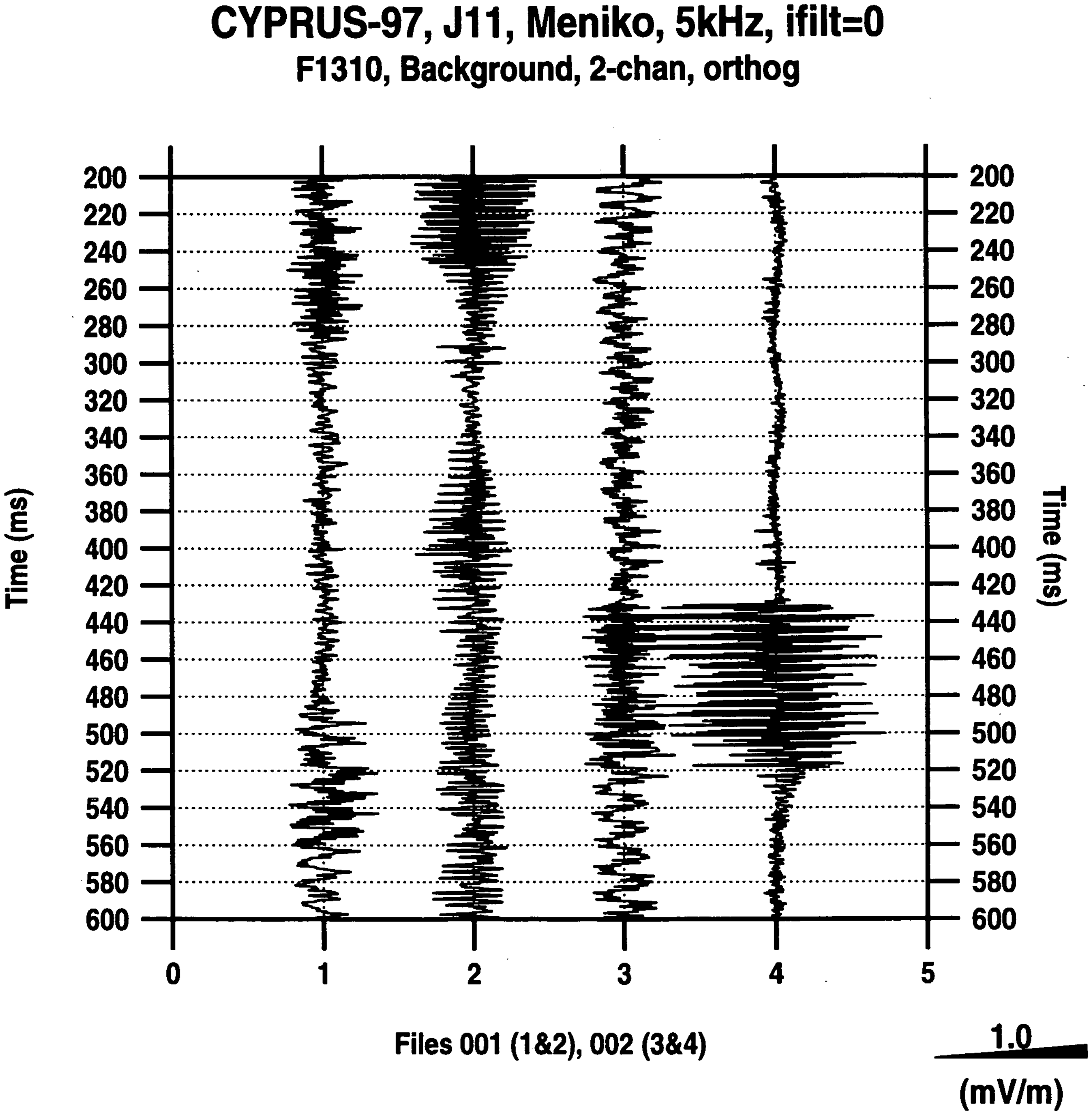

Figure 3.13 Further example of high frequency noise sources - Meniko profile. Background noise tests (no acoustic source) using 10 m orthogonal dipoles. One record (orthogonal channels 1&2), next record (orthogonal channels 3&4).

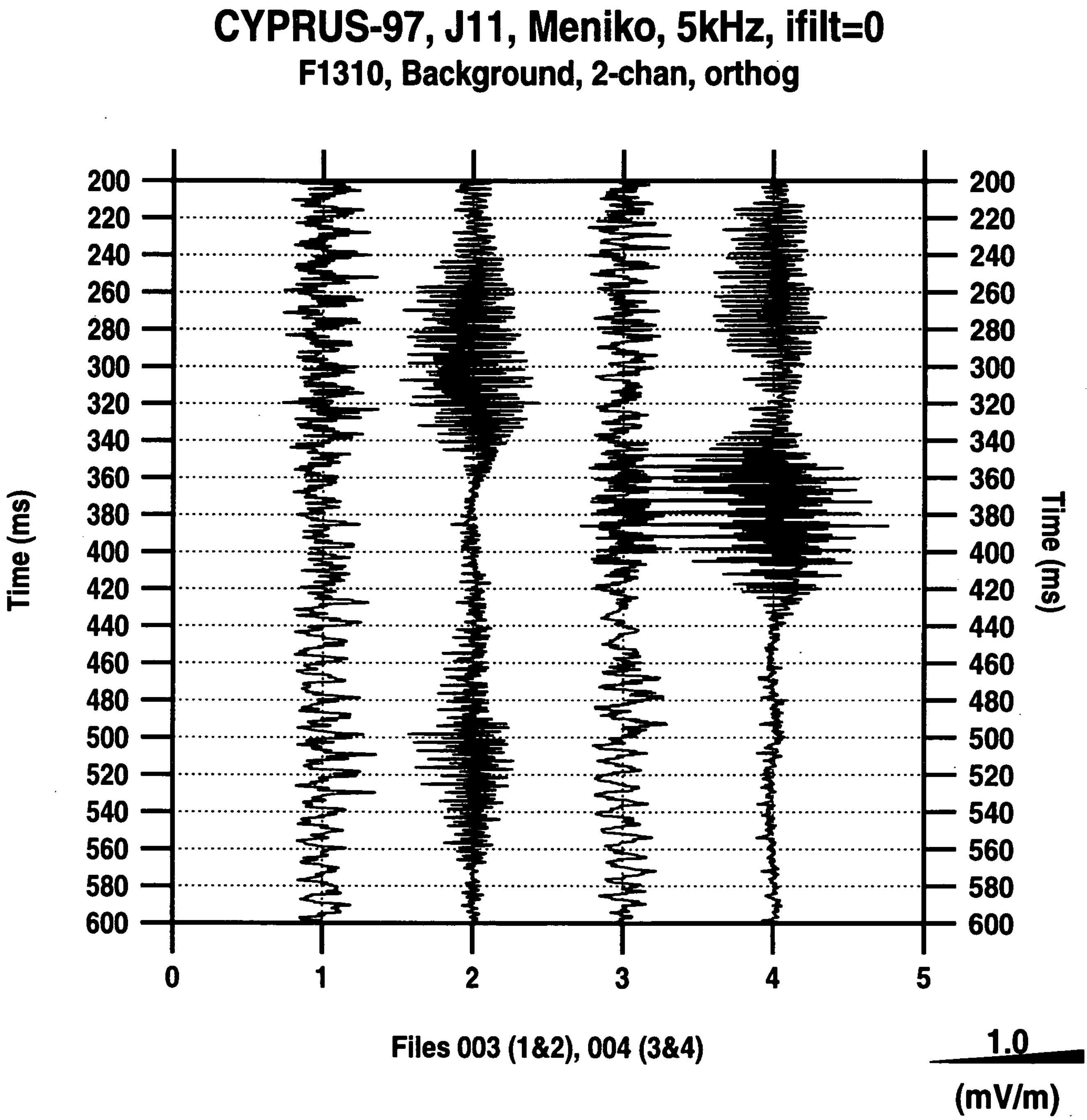

Figure 3.14 Example of frequency spectra of data shown in previous two Figures. Successive background noise tests (no acoustic source).

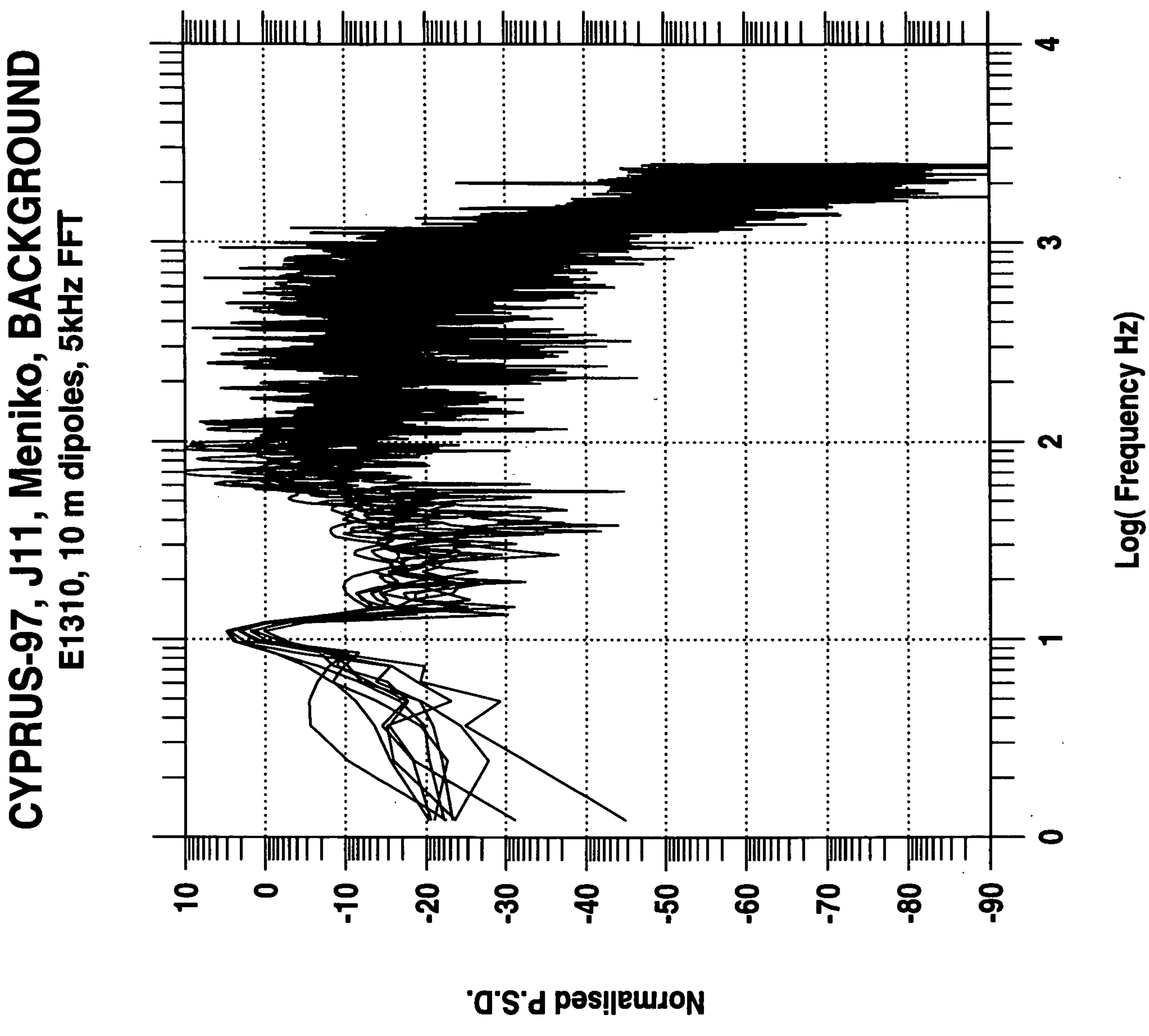

Figure 4.1a 8-channel results. Sounding EP05. Data are trace-normalised. Symmetric channels are shown overlaid (one infill, one line). Dipole centres at +/- 1.5 m (Channel 1), +/- 2.5 m (Channel 2), +/- 3.0 m (Channel 3) and +/- 3.0 m (Channel 4, 4 m dipoles)

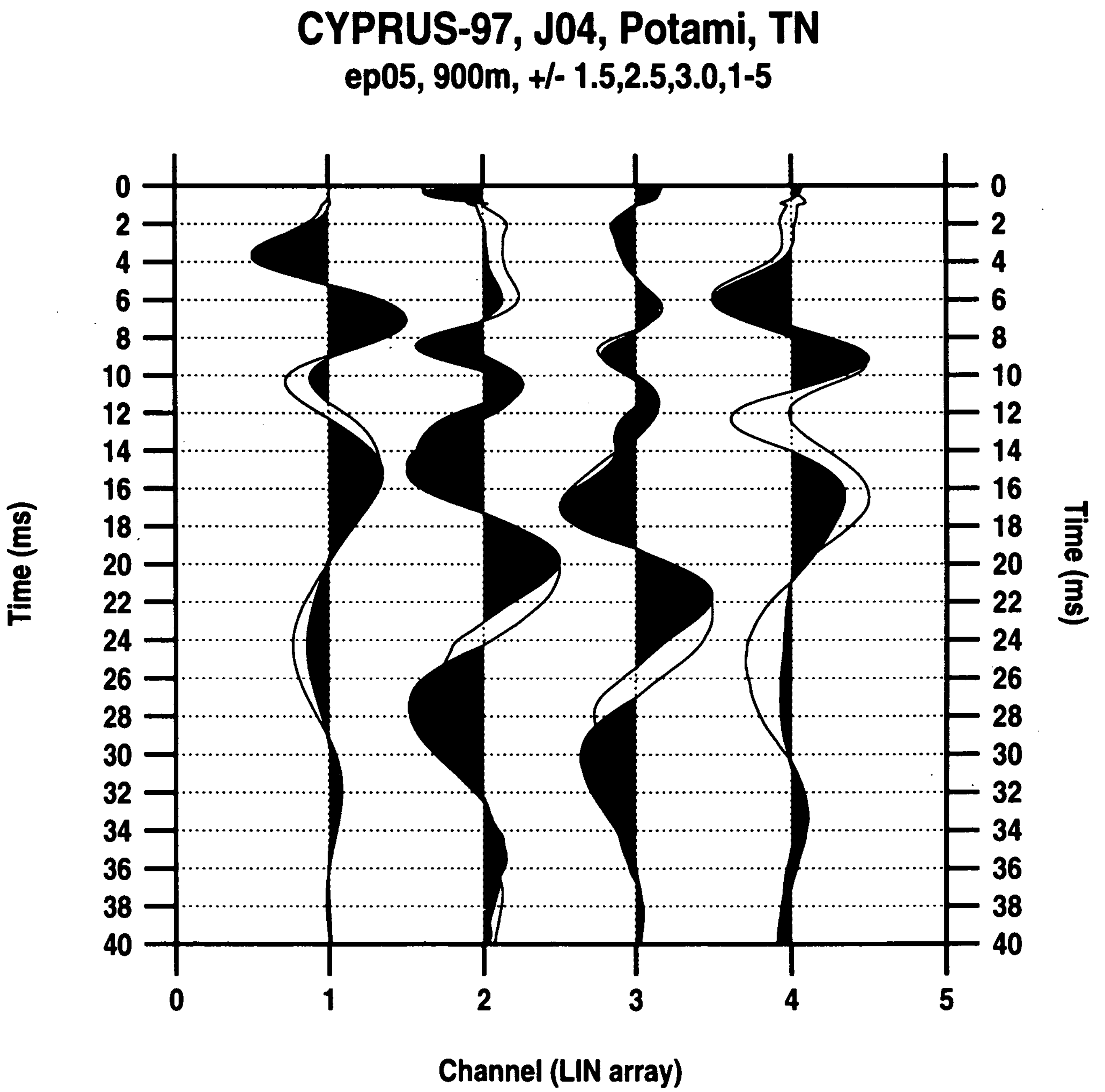

Figure 4.1b 8-channel results. Sounding EP05. Data are true amplitude. Symmetric channels are shown overlaid (one infill, one line). Dipole centres at +/- 1.5 m (Channel 1), +/- 2.5 m (Channel 2), +/- 3.0 m (Channel 3) and +/- 3.0 m (Channel 4, 4 m dipoles)

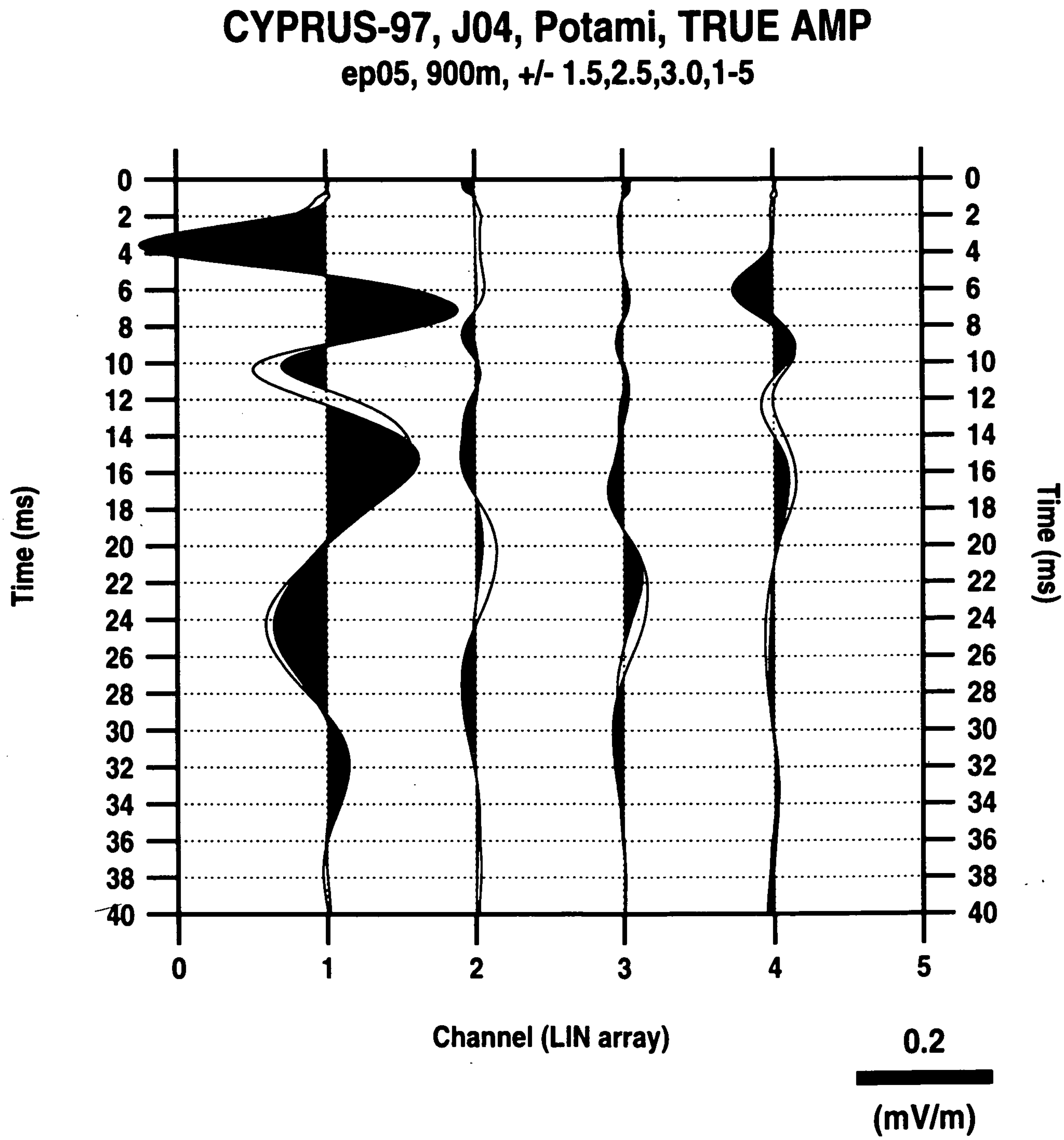

Figure 4.2 8-channel results. Sounding EP05. Data are true amplitude. Symmetric channels are shown overlaid (one infill, one line). Dipole centres at +/- 1.5 m (Channel 1), +/- 2.5 m (Channel 2), +/- 3.0 m (Channel 3) and +/- 3.0 m (Channel 4, 4 m dipoles). Time interval 100-140 ms.

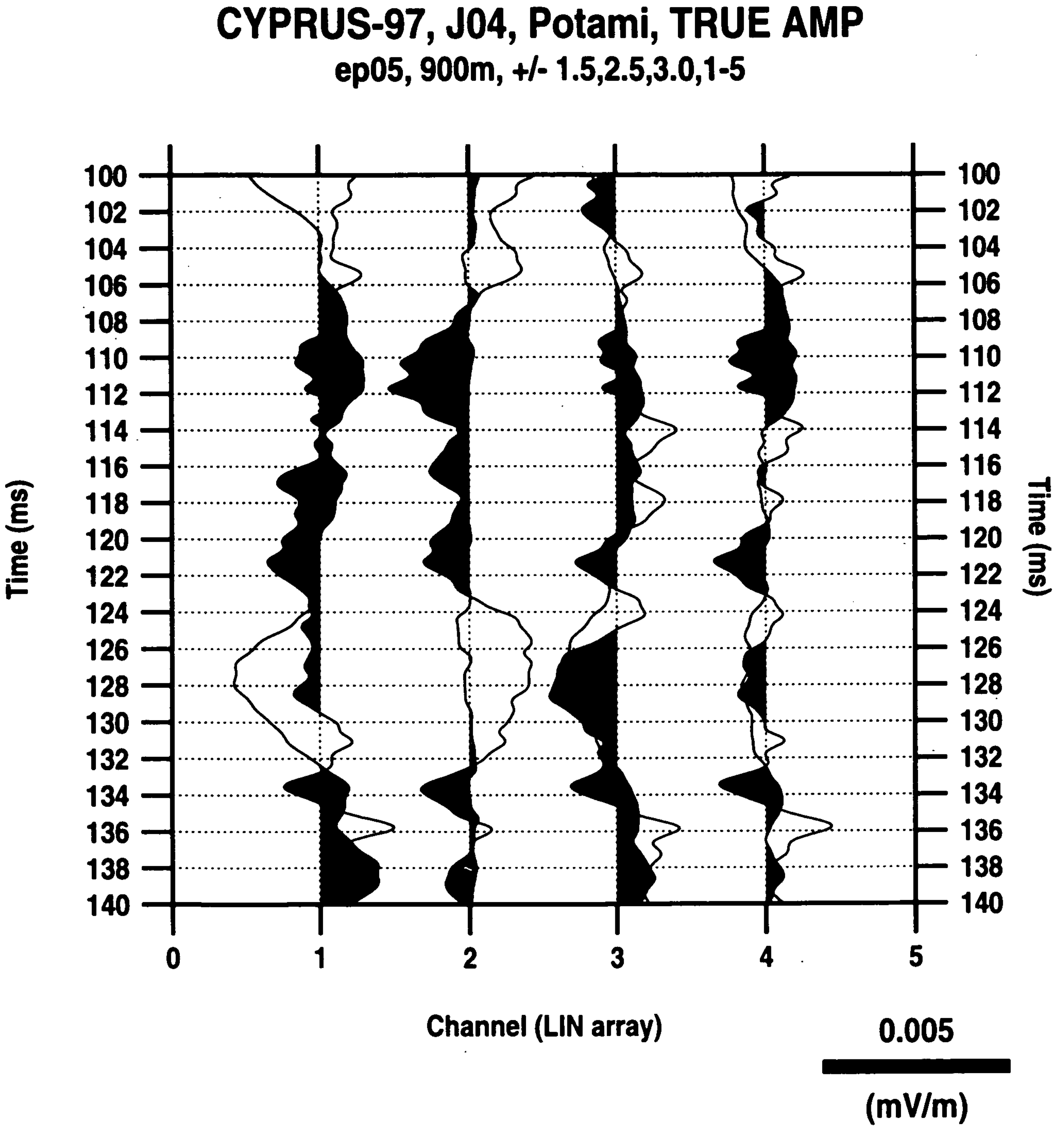

Figure 4.3 8-channel results. Sounding EP05. Data are true amplitude. Symmetric channels are shown overlaid (one infill, one line). Dipole centres at +/- 1.5 m (Channel 1), +/- 2.5 m (Channel 2), +/- 3.0 m (Channel 3) and +/- 3.0 m (Channel 4, 4 m dipoles). Time interval 200-240 ms.

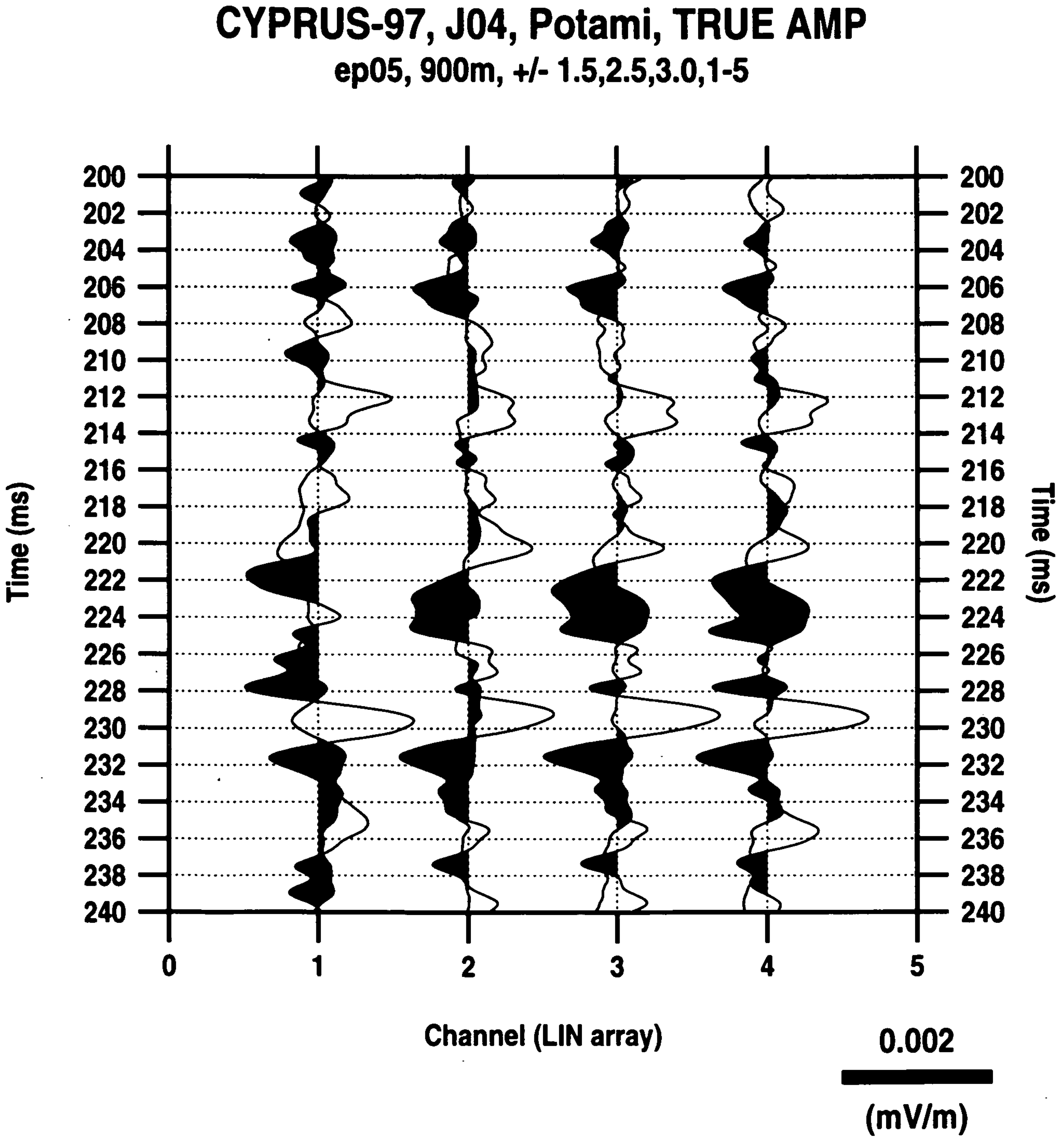

Figure 4.4 8-channel results. Sounding EP11. Data are true amplitude. Symmetric channels are shown overlaid (one infill, one line). Dipole centres at +/- 1.5 m (Channel 1), +/- 2.5 m (Channel 2), +/- 3.0 m (Channel 3) and +/- 2.25 m (Channel 4, 4 m dipoles). Time interval 100-140 ms.

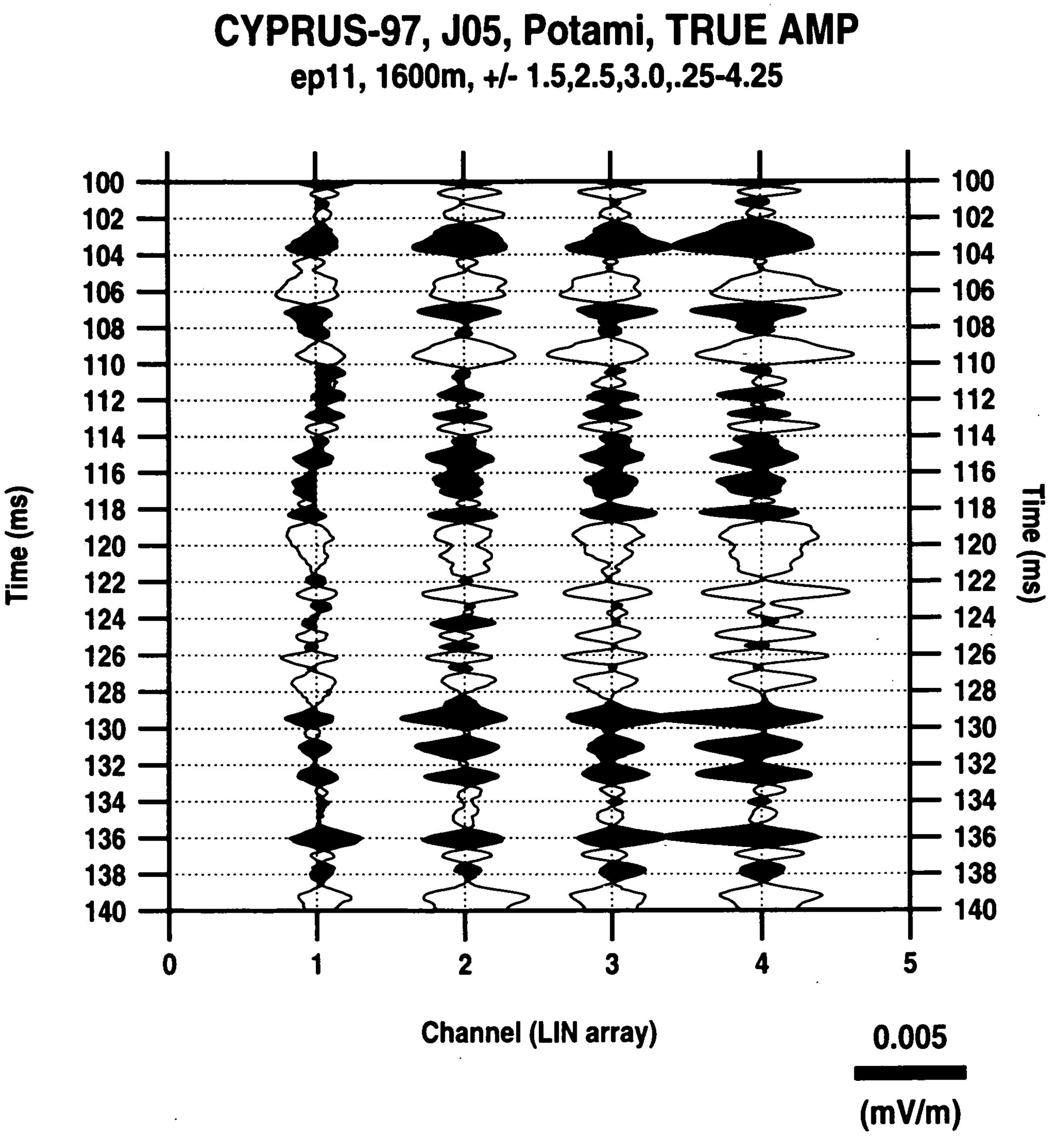

Figure 5.1 Example of results of acoustic moveout experiment. Potami profile, 200 m.

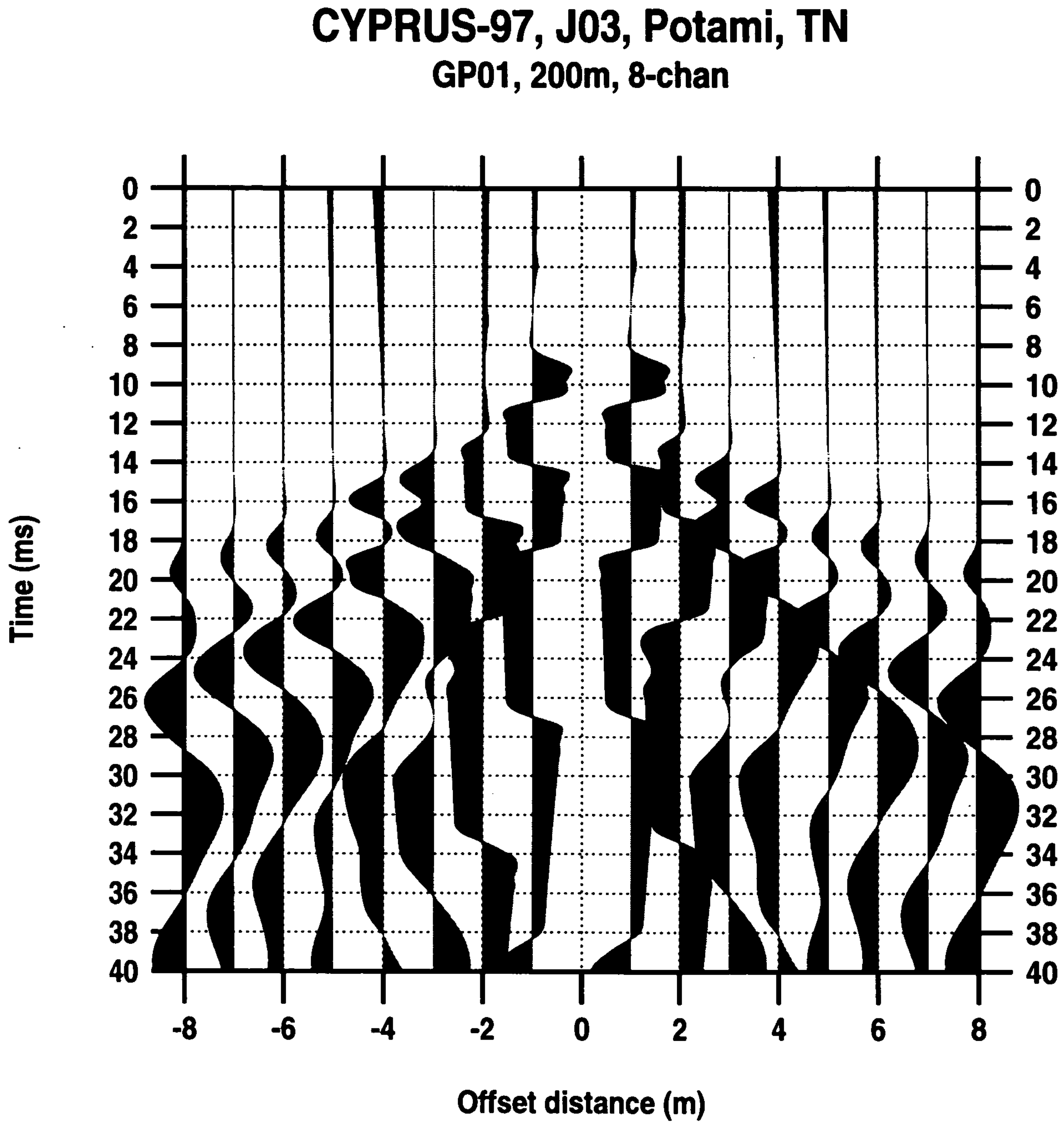

Figure 5.2a Example of maximum entropy spectra of acoustic moveout data. Record interval 0 to 200 ms. Results from 8 channels of data overlaid.

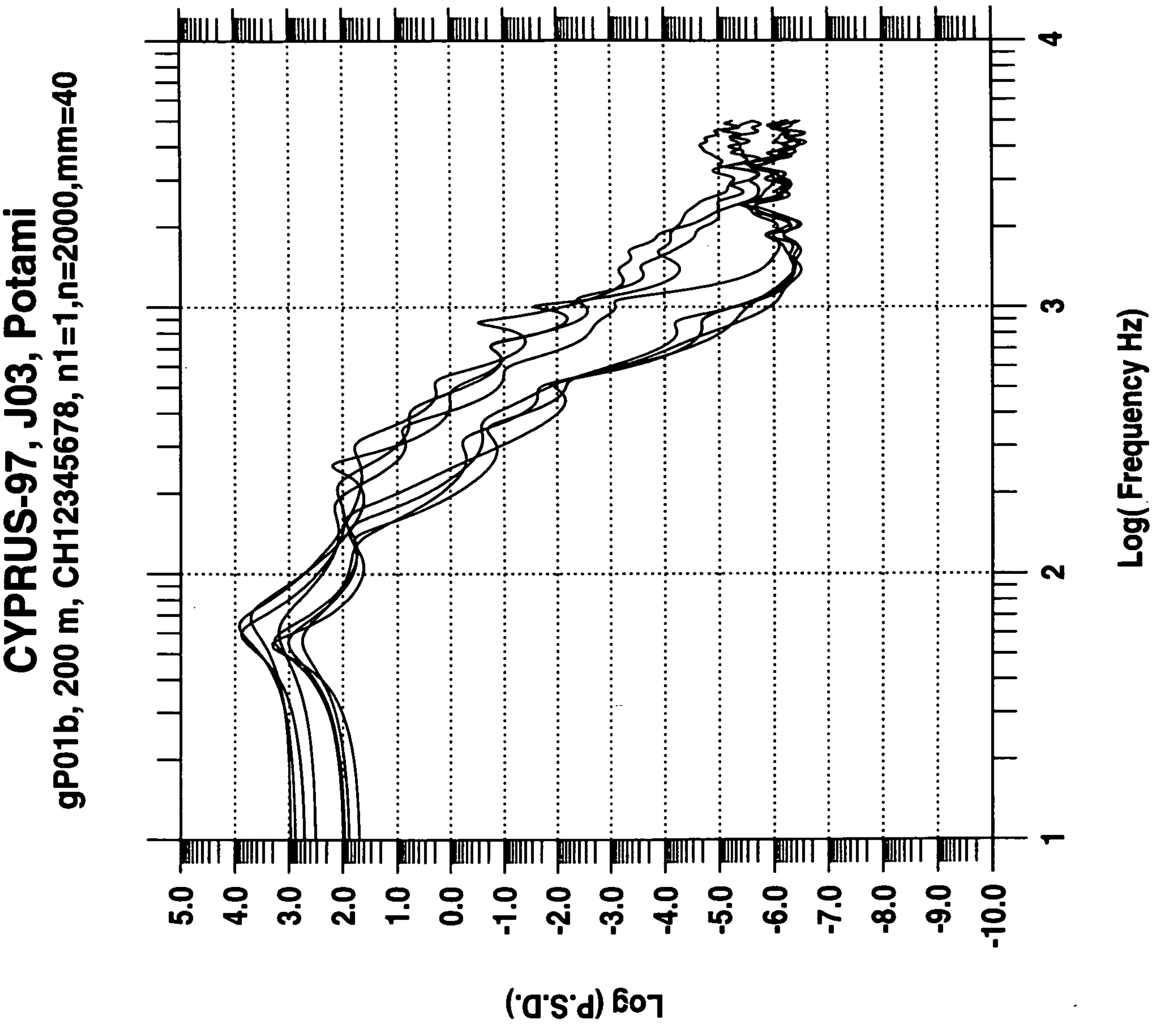

Figure 5.2b Example of maximum entropy spectra of acoustic moveout data. Record interval 200 to 400 ms. Results from 8 channels of data overlaid.

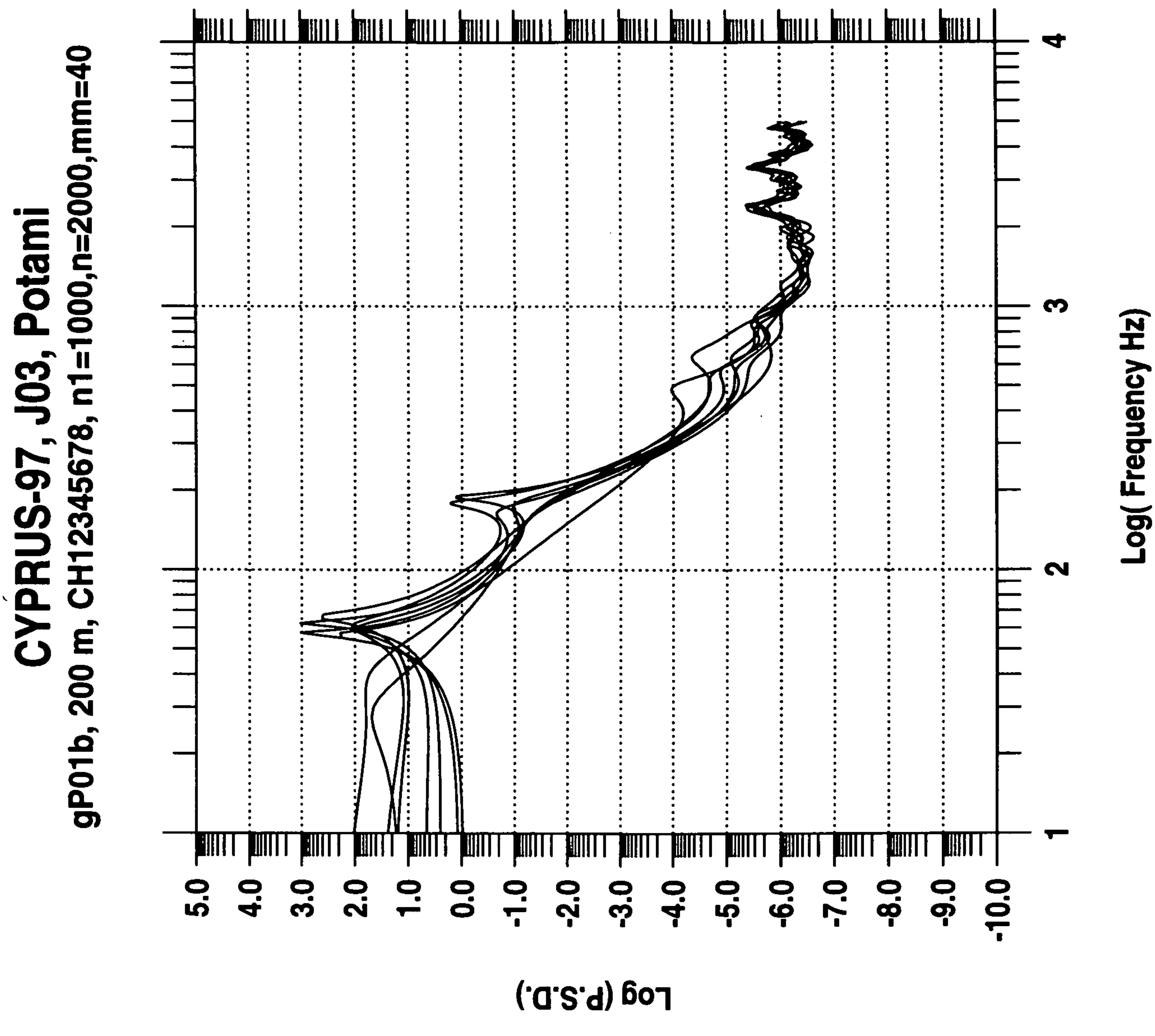

Figure 6.1a Example of profile data. Potami location 1210 m. Channel 1 (single channel) data obtained at 5 m intervals. Data are trace normalised.

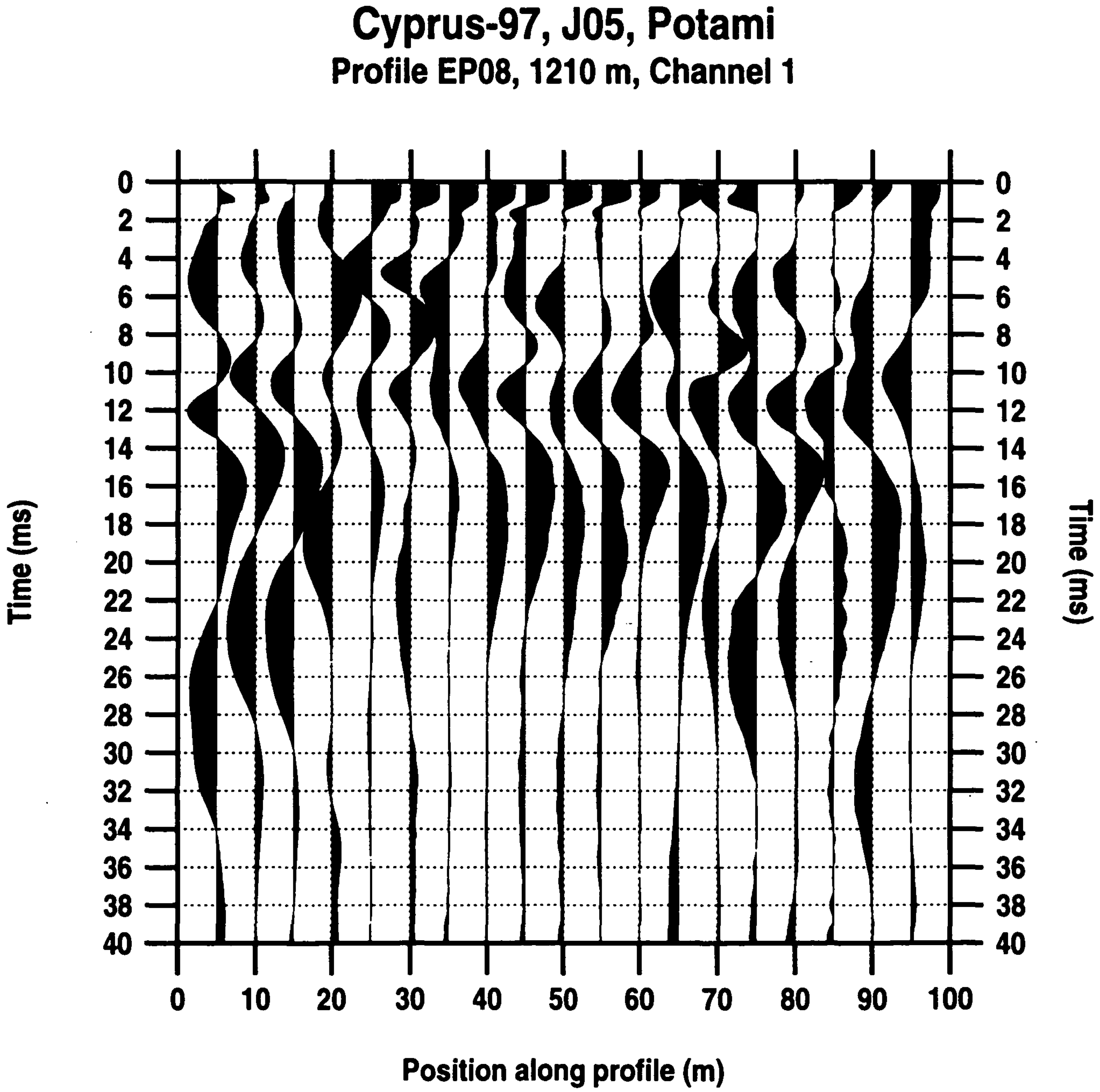

Figure 6.1b Example of profile data. Potami location 1210 m. Channel 2 (single channel) data obtained at 5 m intervals. Data are trace normalised.

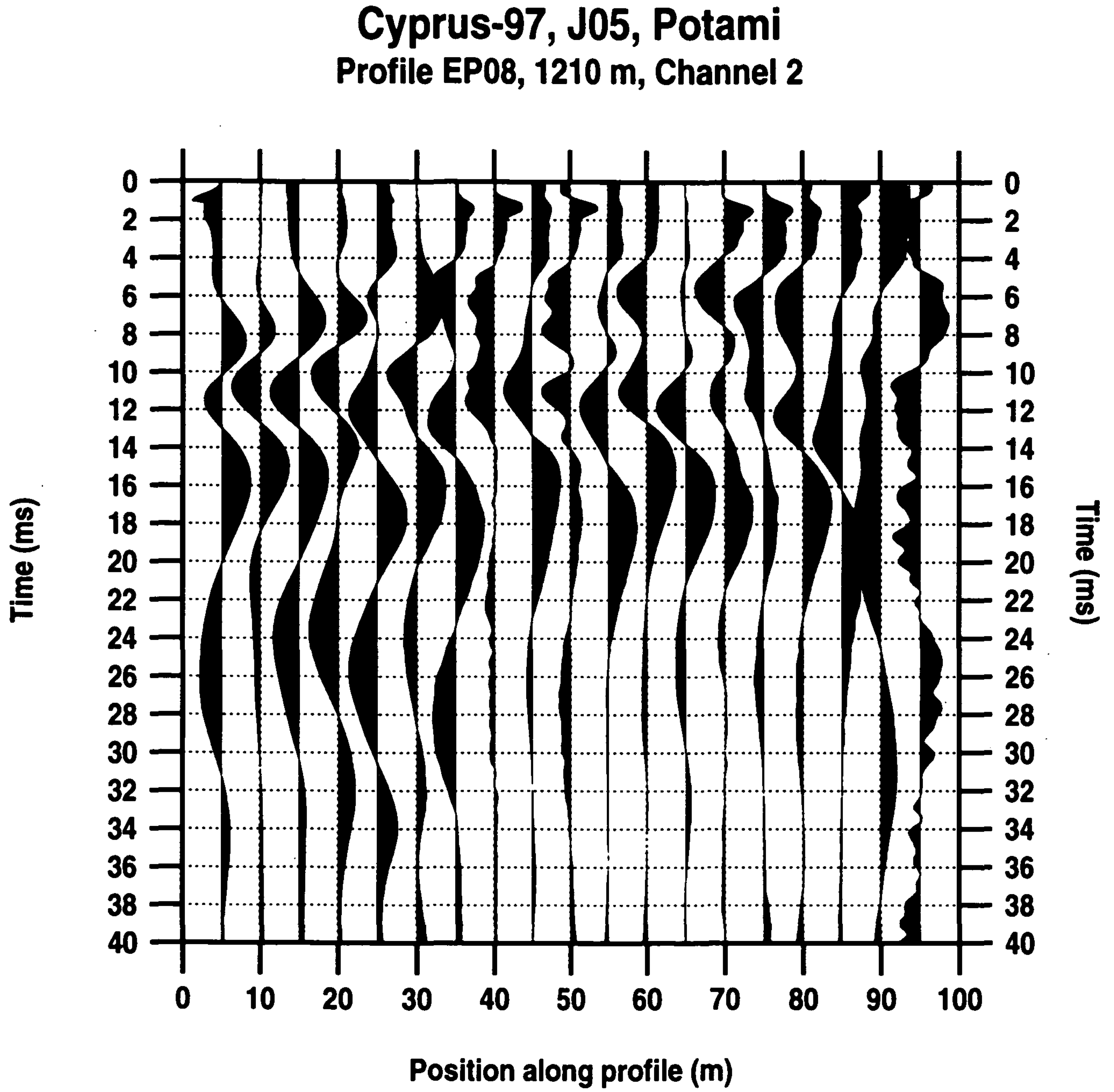

Figure 7.1 8-channel results. Sounding EP19. Data are trace normalised. Symmetric channels are shown overlaid. Dipole centres at +/- 1.0 m (Channel 1), +/- 2.0 m (Channel 2), +/- 3.0 m (Channel 3) and +/- 2.25 m (Channel 4, 4 m dipoles). Time interval 0-80 ms.

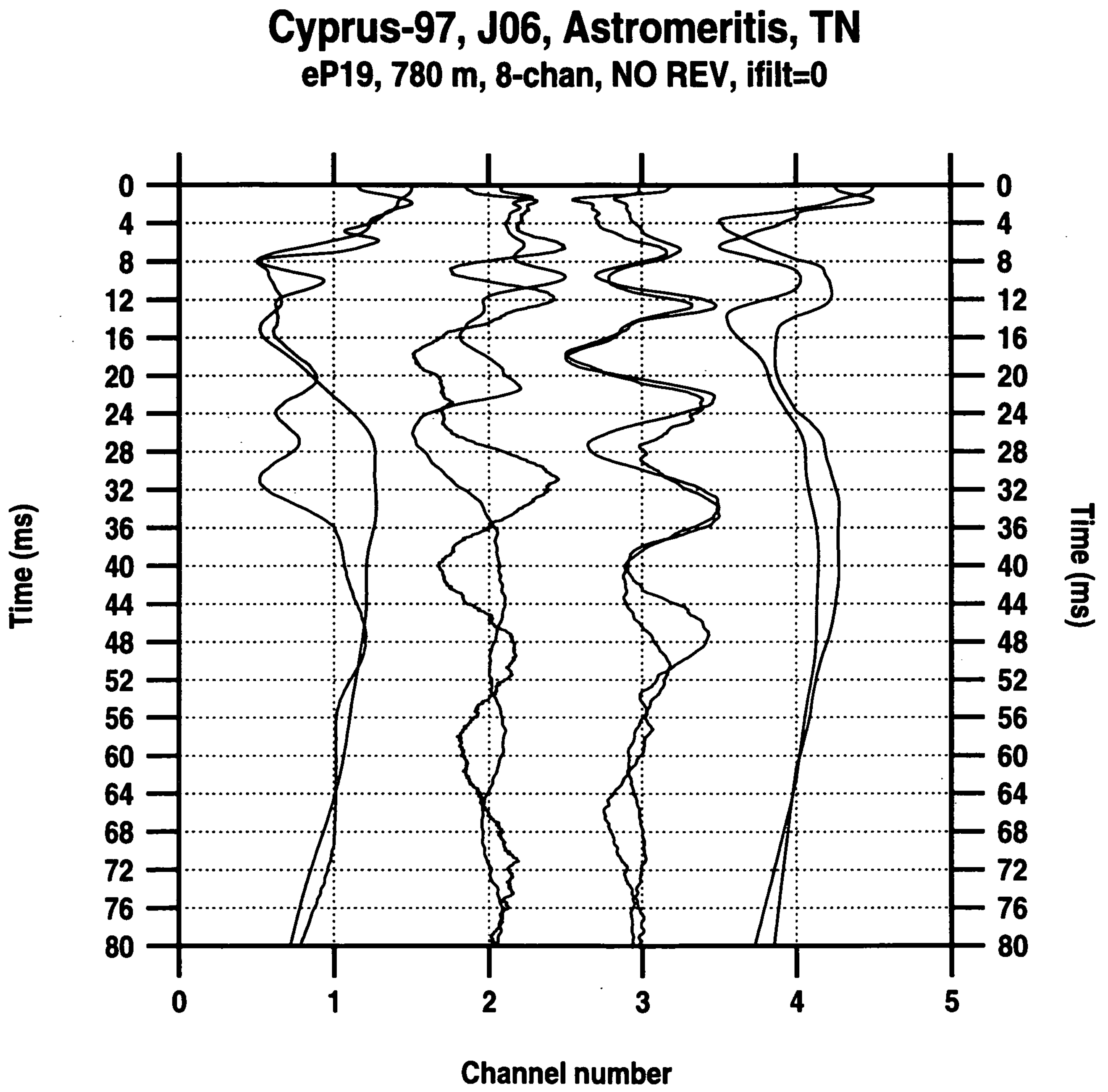

Figure 7.2a Potami profile, first seven soundings (200 to 1100 m along profile). Inner two shot-symmetric channels of each sounding (one infill and one line) are overlaid. Trace-normalised data. Time interval 0 to 40 ms.

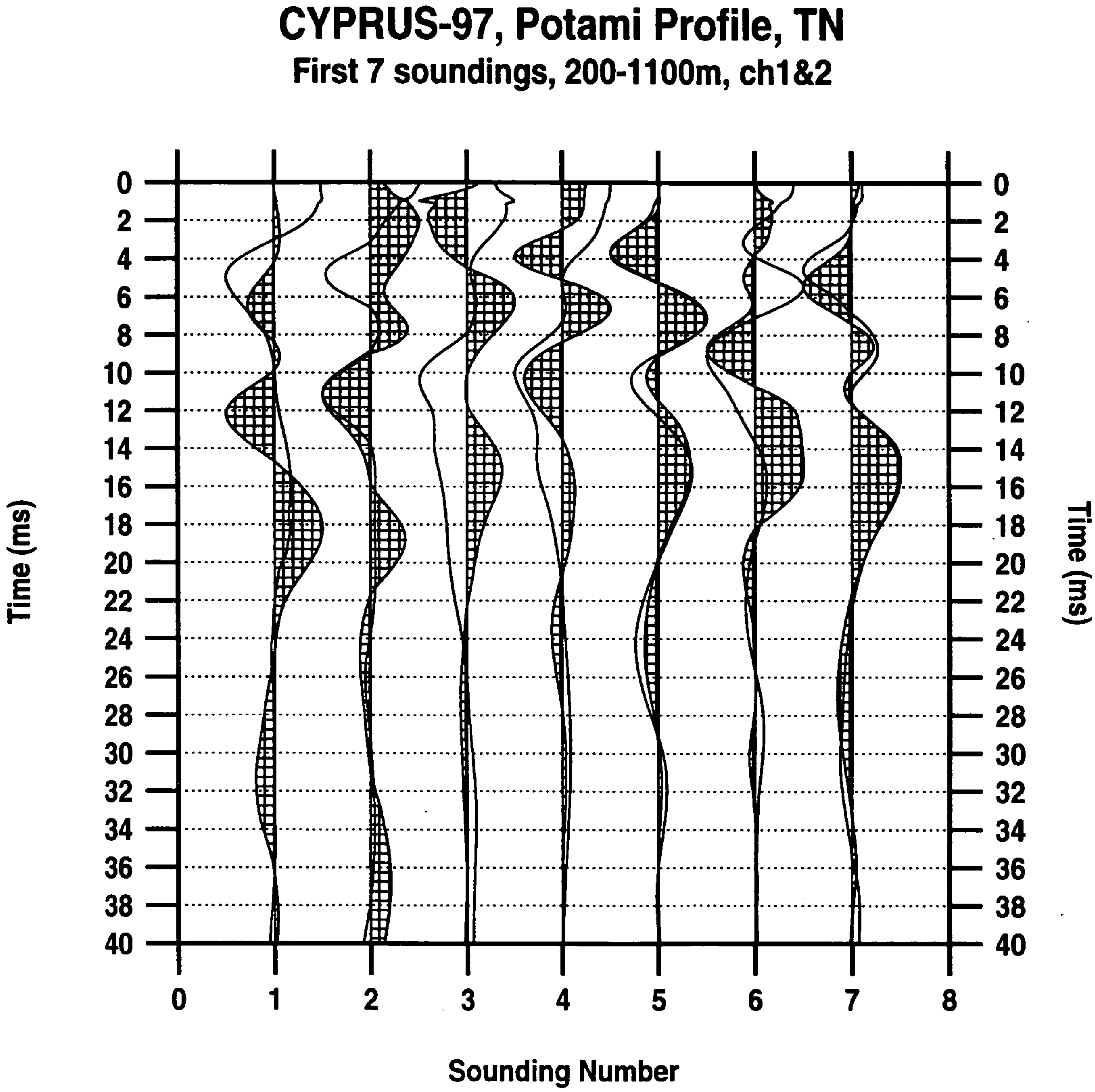

Figure 7.2b Potami profile, first seven soundings (200 to 1100 m along profile). Inner two shot-symmetric channels of each sounding (one infill and one line) are overlaid. Trace-normalised data. Time interval 40 to 80 ms.

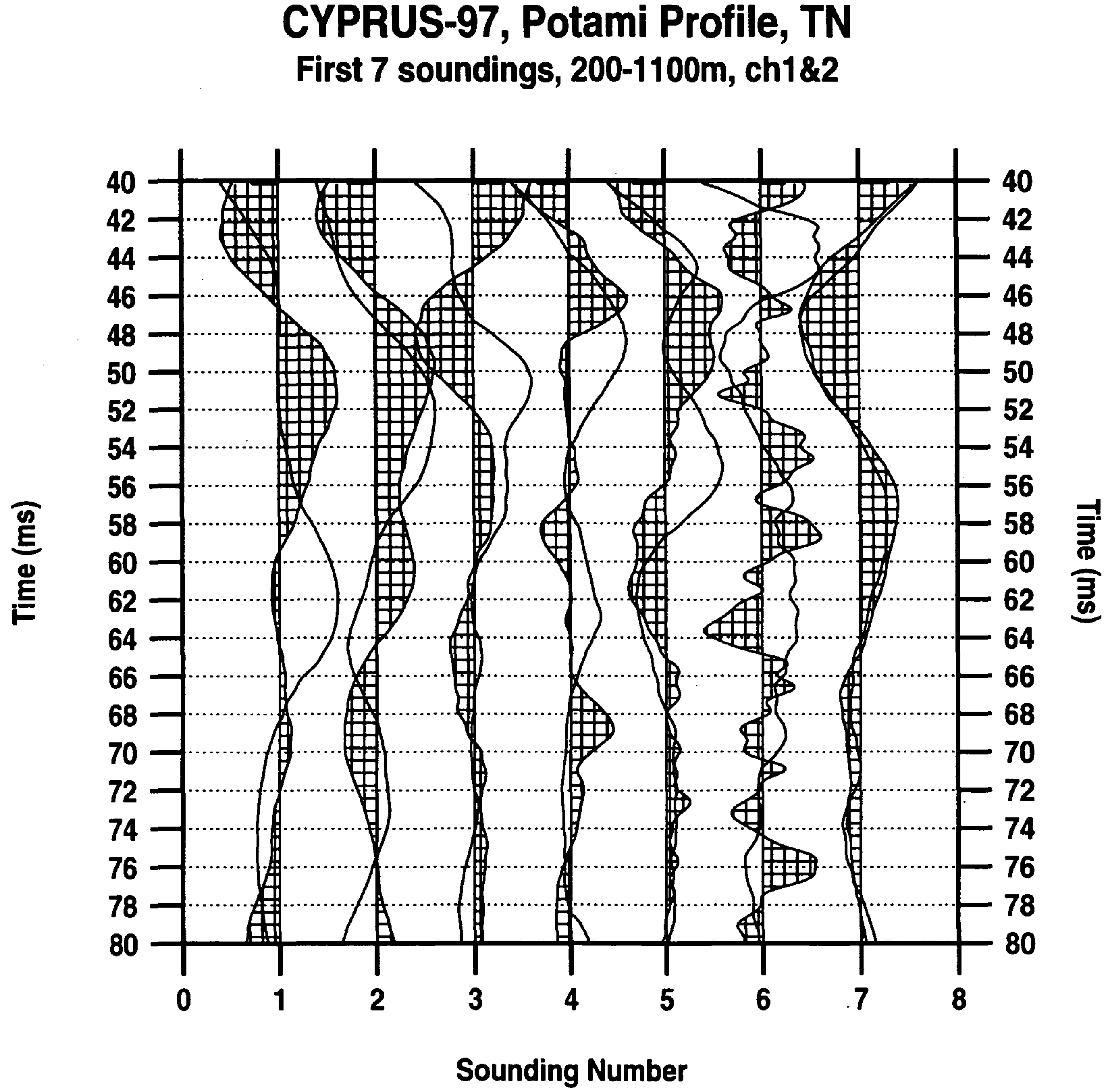

Figure 7.2c Potami profile, first seven soundings (200 to 1100 m along profile). Inner two shot-symmetric channels of each sounding (one infill and one line) are overlaid. Trace-normalised data. Time interval 80 to 160 ms.

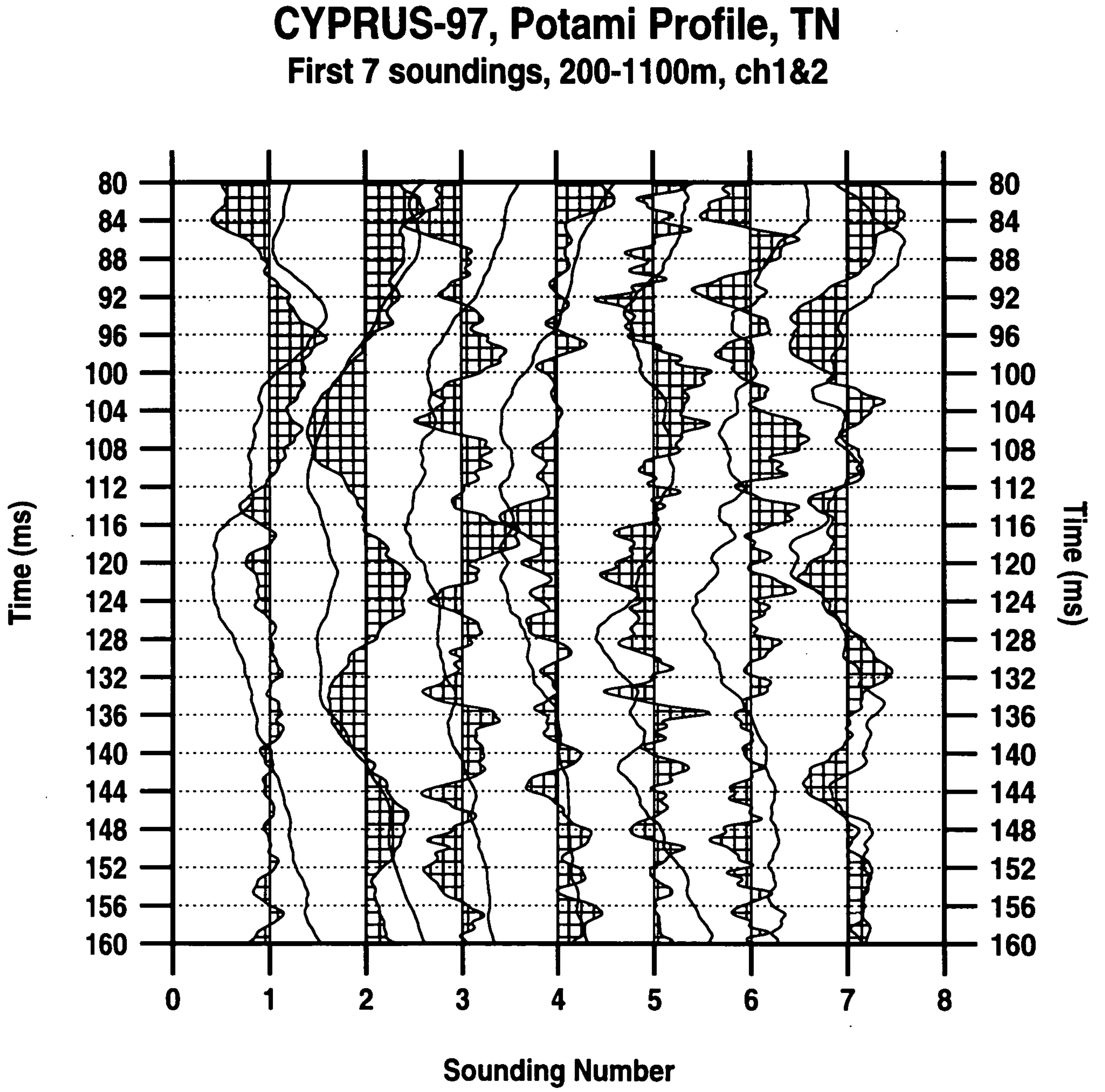

Figure 7.2d Potami profile, first seven soundings (200 to 1100 m along profile). Inner two shot-symmetric channels of each sounding (one infill and one line) are overlaid. Trace-normalised data. Time interval 160 to 240 ms.

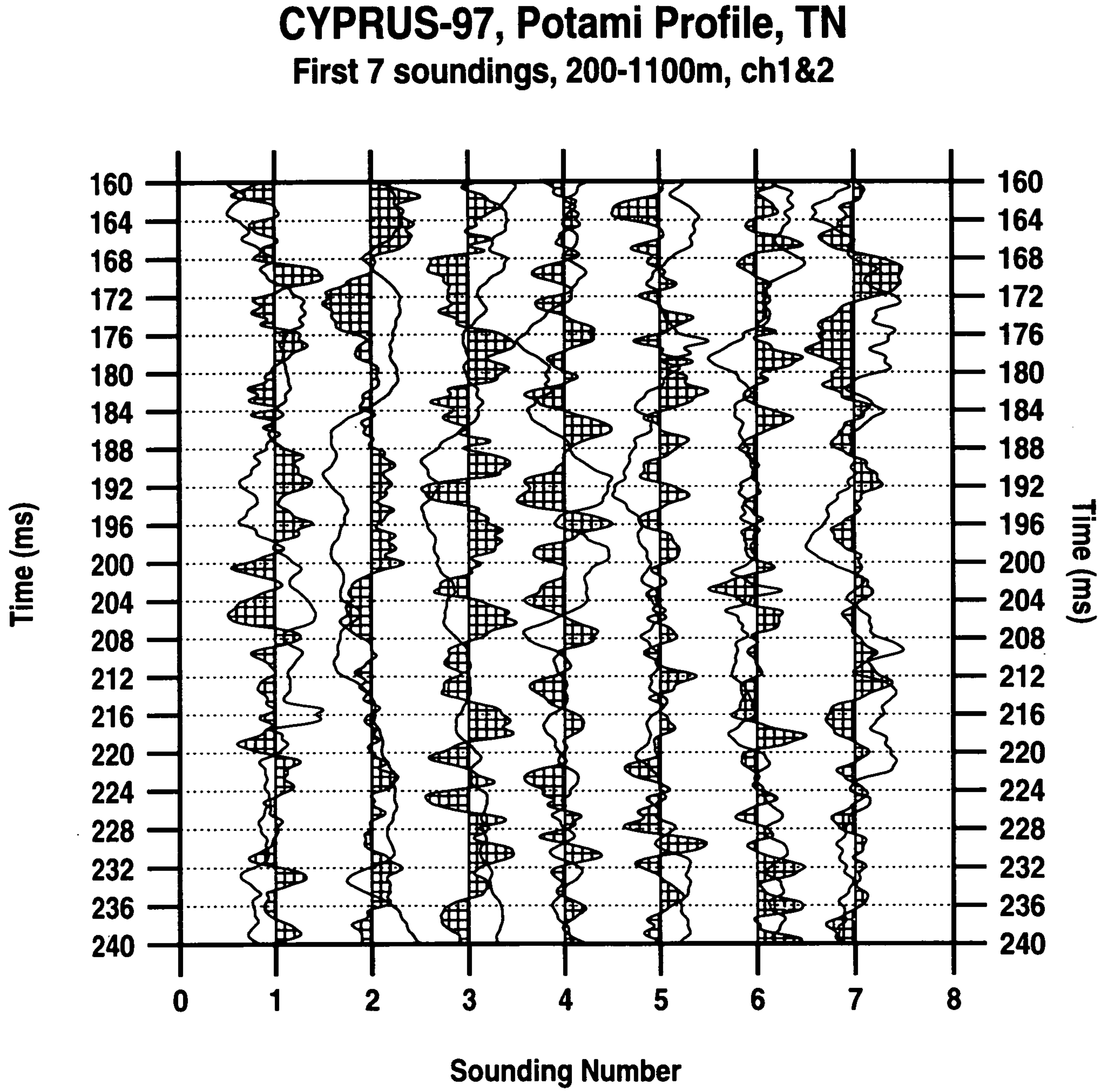

Figure 7.3a Potami profile, second seven soundings (1100 to 1800 m along profile). Inner two shot-symmetric channels of each sounding (one infill and one line) are overlaid. Trace-normalised data. Time interval 0 to 40 ms.

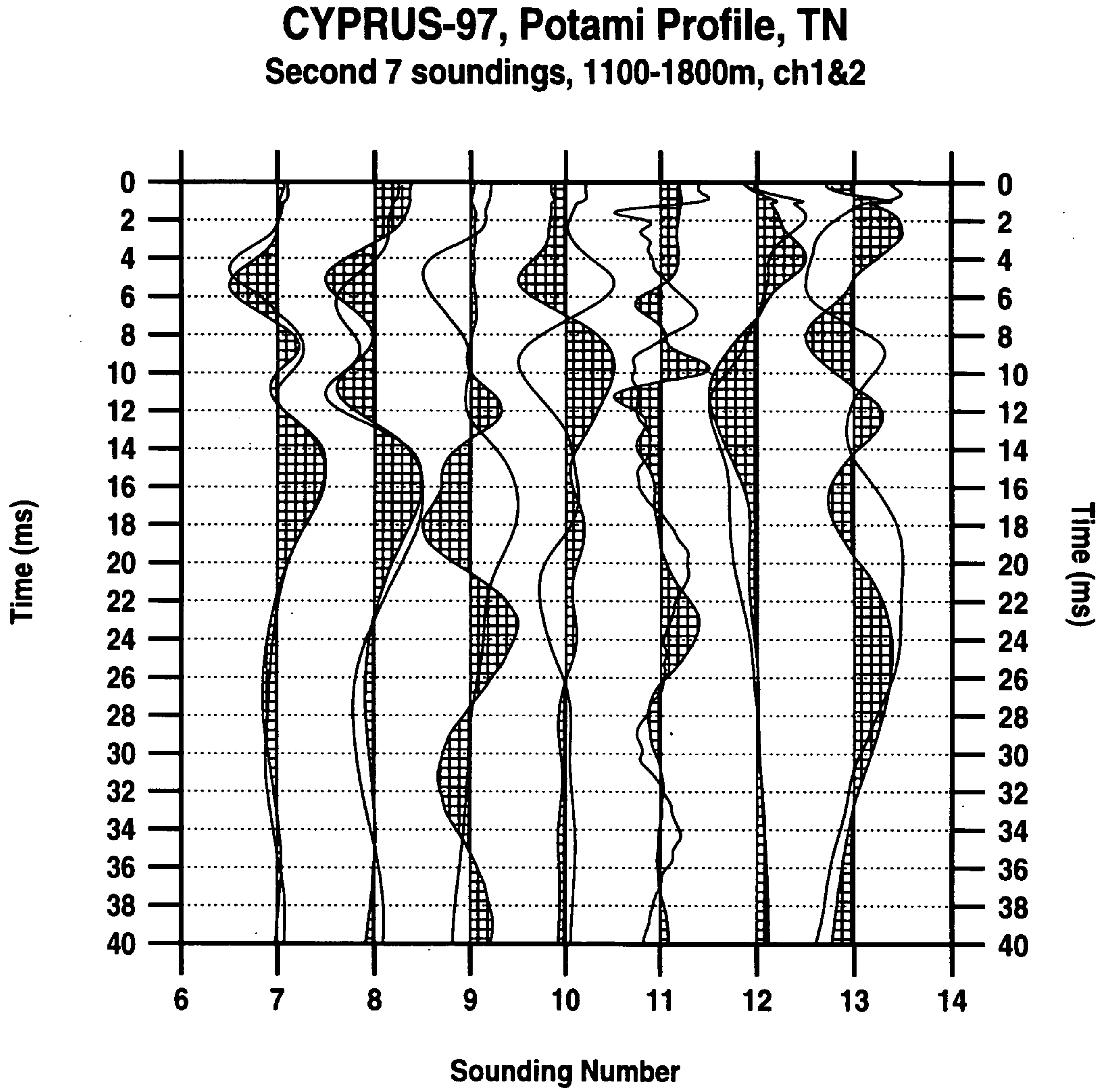

Figure 7.3b Potami profile, second seven soundings (1100 to 1800 m along profile). Inner two shot-symmetric channels of each sounding (one infill and one line) are overlaid. Trace-normalised data. Time interval 40 to 80 ms.

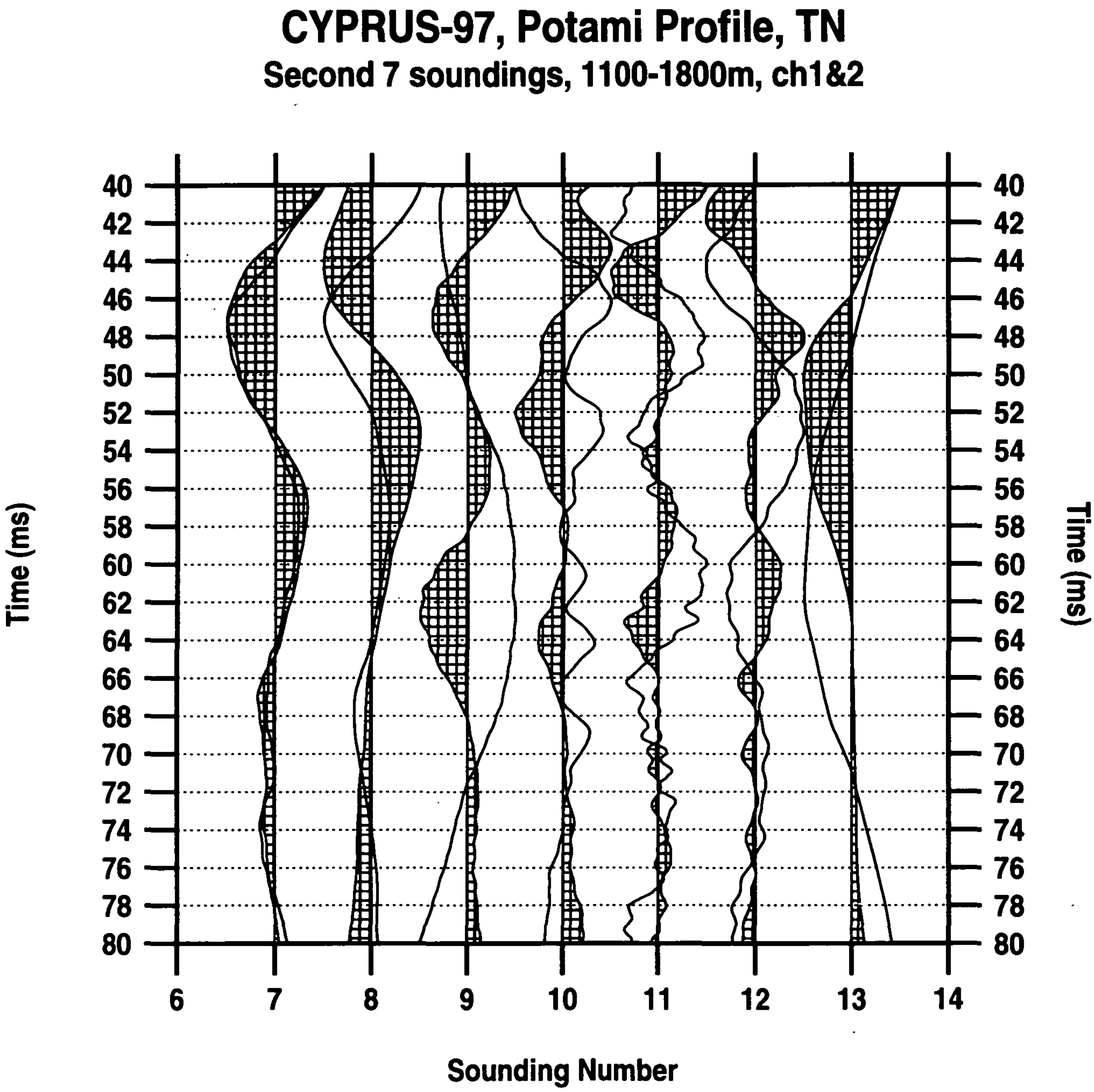

Figure 7.3c Potami profile, second seven soundings (1100 to 1800 m along profile). Inner two shot-symmetric channels of each sounding (one infill and one line) are overlaid. Trace-normalised data. Time interval 80 to 160 ms.

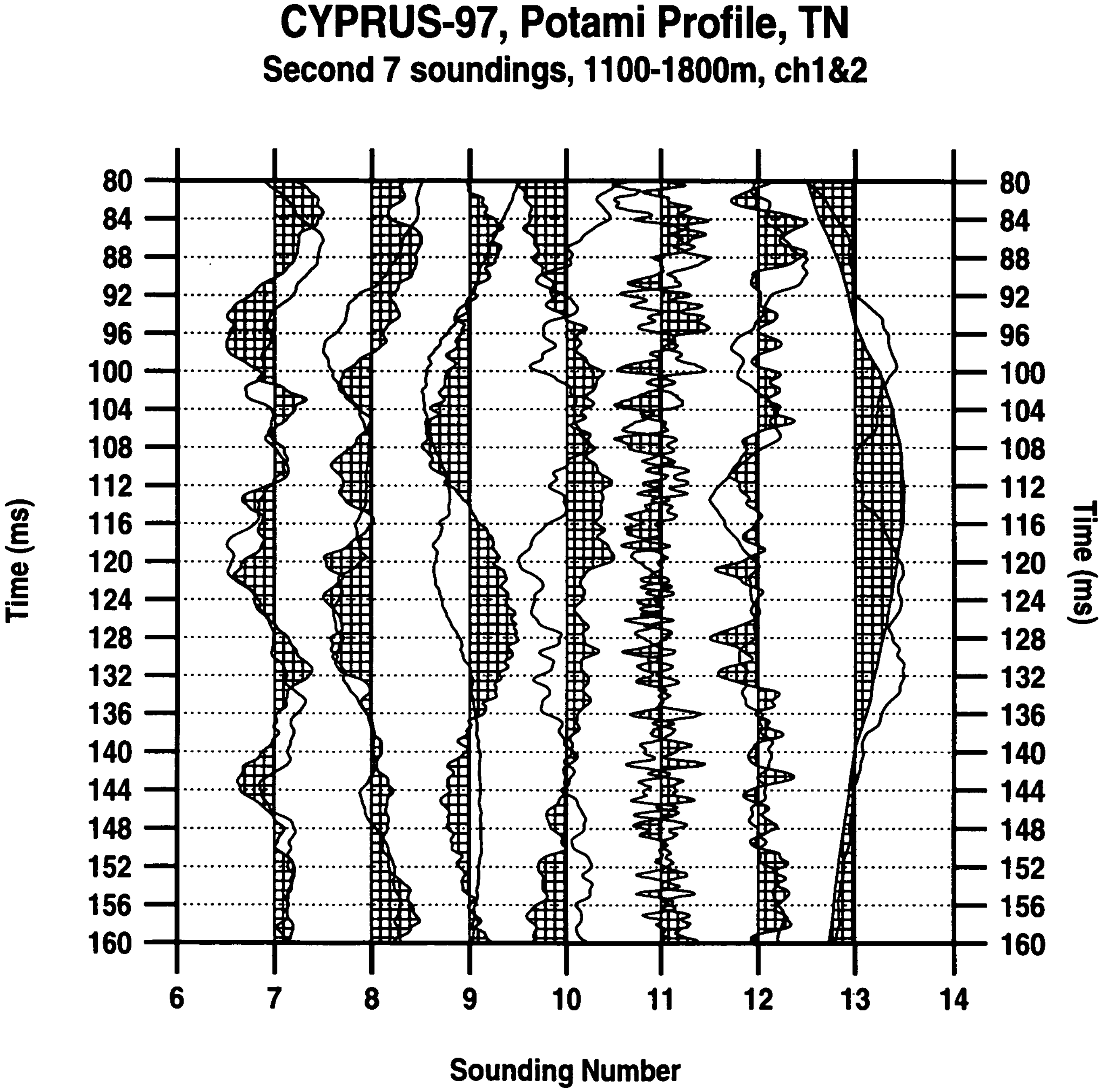

Figure 7.3d Potami profile, second seven soundings (1100 to 1800 m along profile). Inner two shot-symmetric channels of each sounding (one infill and one line) are overlaid. Trace-normalised data. Time interval 160 to 240 ms.

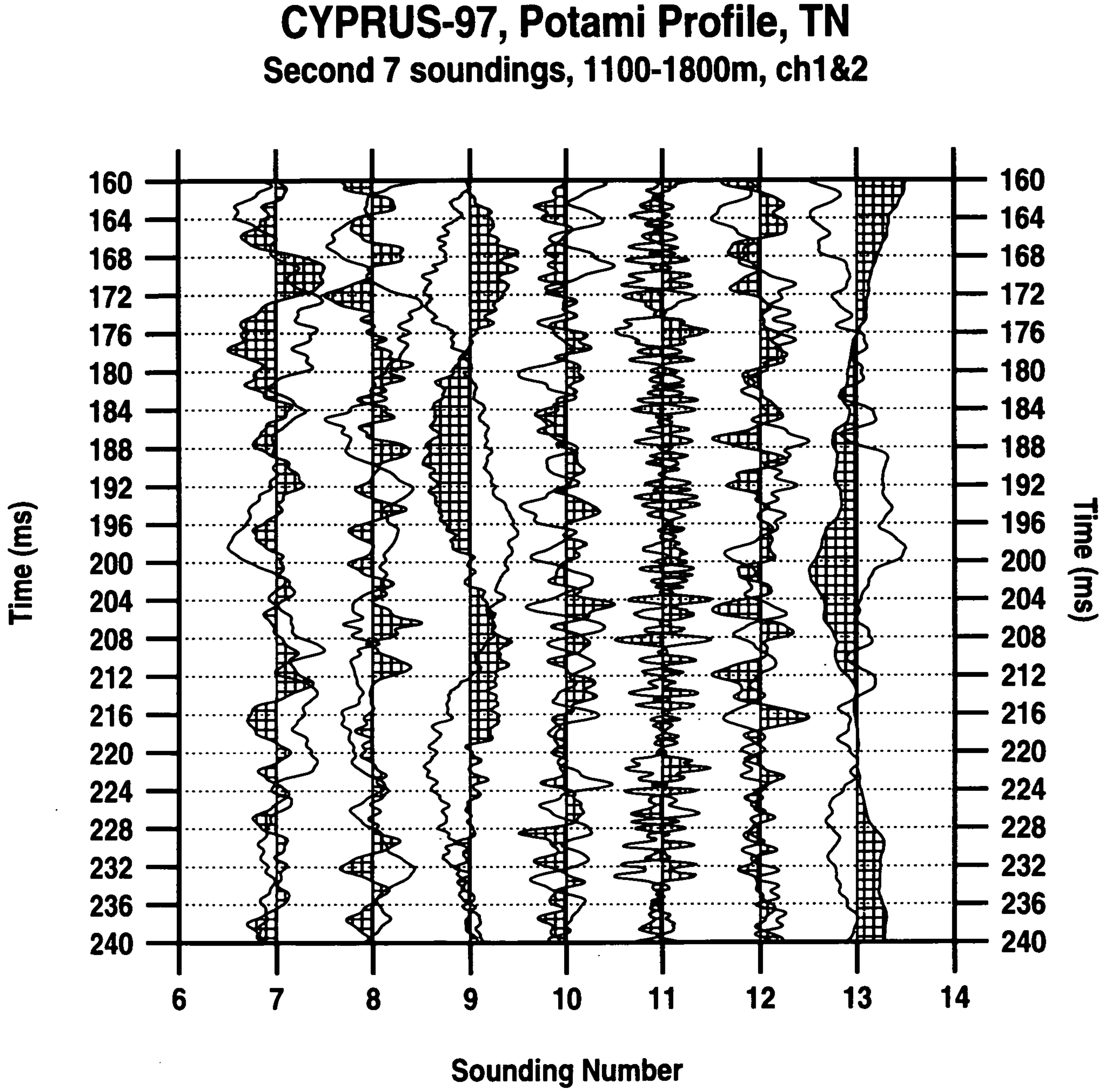

Figure 7.4a Astromeritis profile, first six soundings (70 to 780 m along profile). Inner two shot-symmetric channels of each sounding (one infill and one line) are overlaid. Trace-normalised data. Time interval 0 to 40 ms.

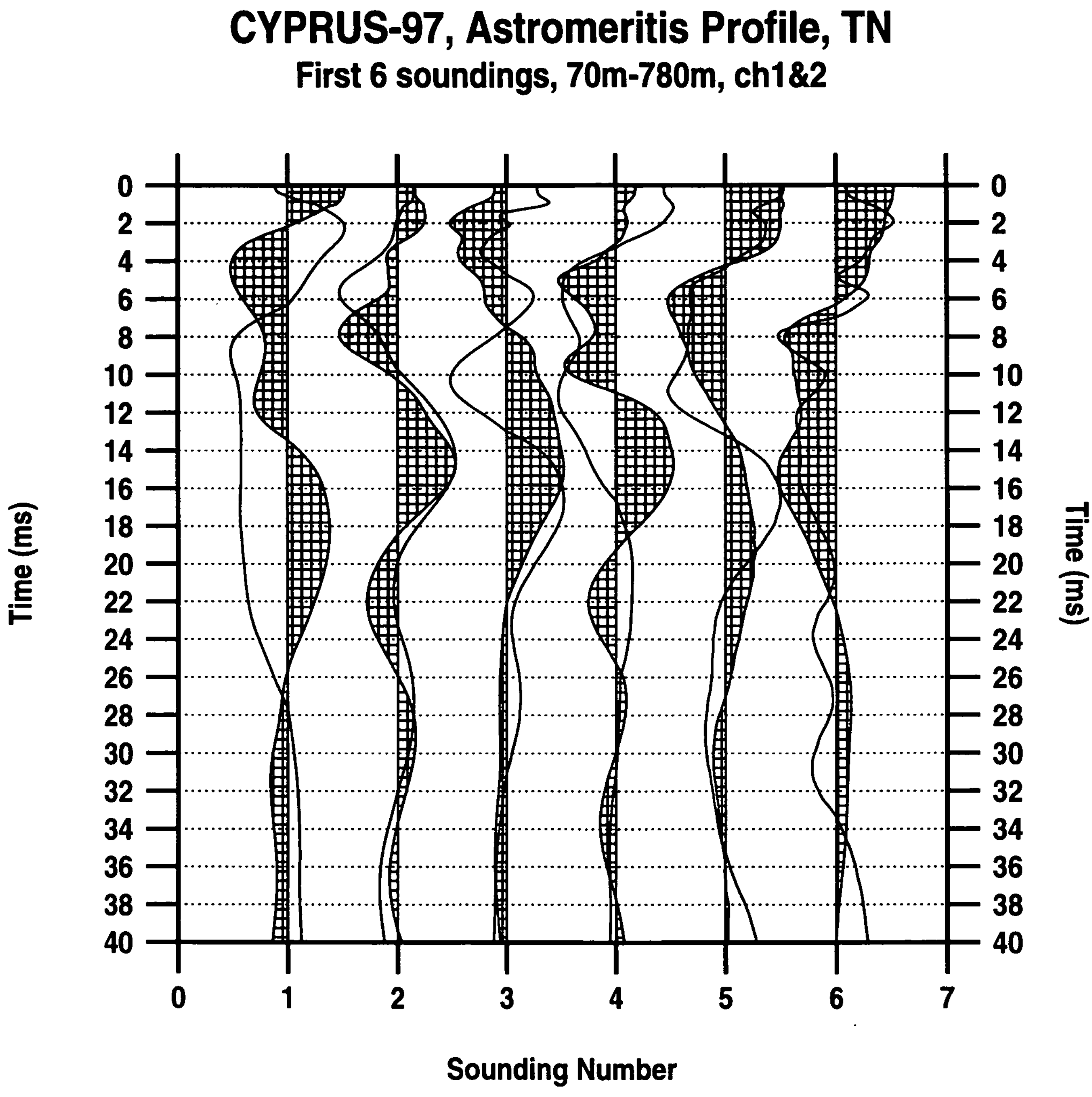

Figure 7.4b Astromeritis profile, first six soundings (70 to 780 m along profile). Inner two shot-symmetric channels of each sounding (one infill and one line) are overlaid. Trace-normalised data. Time interval 40 to 80 ms.

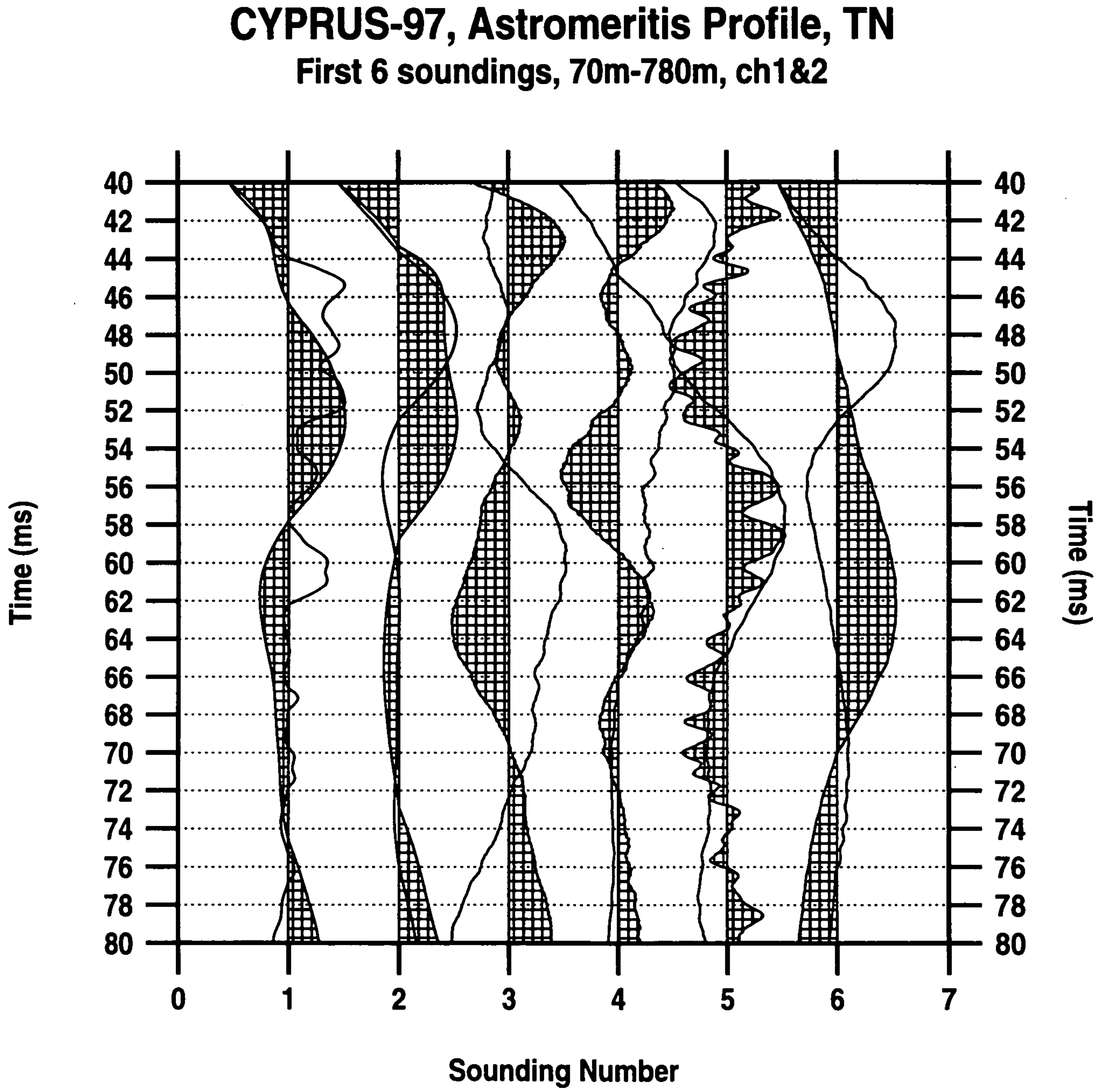

Figure 7.4c Astromeritis profile, first six soundings (70 to 780 m along profile). Inner two shot-symmetric channels of each sounding (one infill and one line) are overlaid. Trace-normalised data. Time interval 80 to 160 ms.

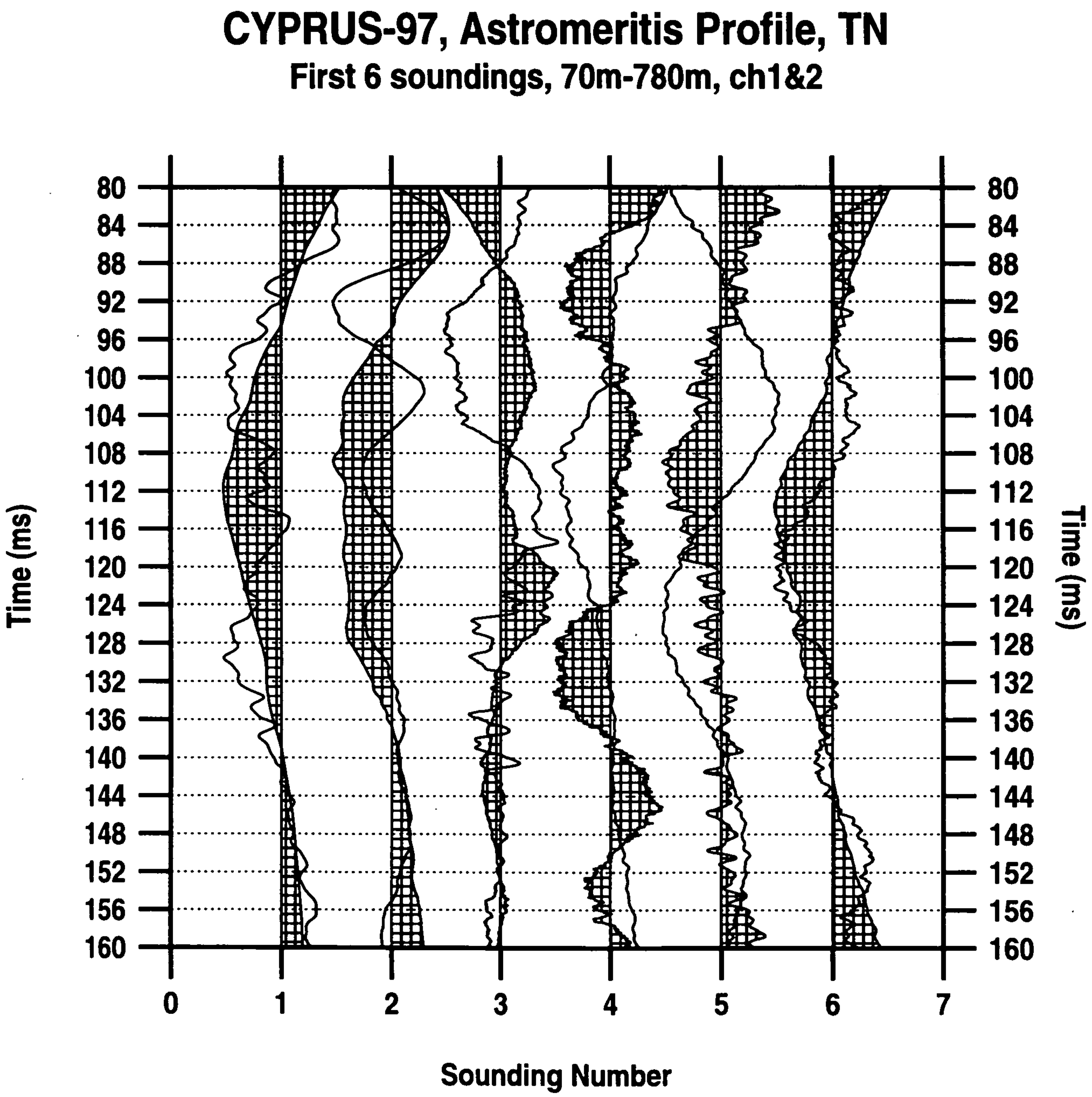

Figure 7.4d Astromeritis profile, first six soundings (70 to 780 m along profile). Inner two shot-symmetric channels of each sounding (one infill and one line) are overlaid. Trace-normalised data. Time interval 160 to 240 ms.

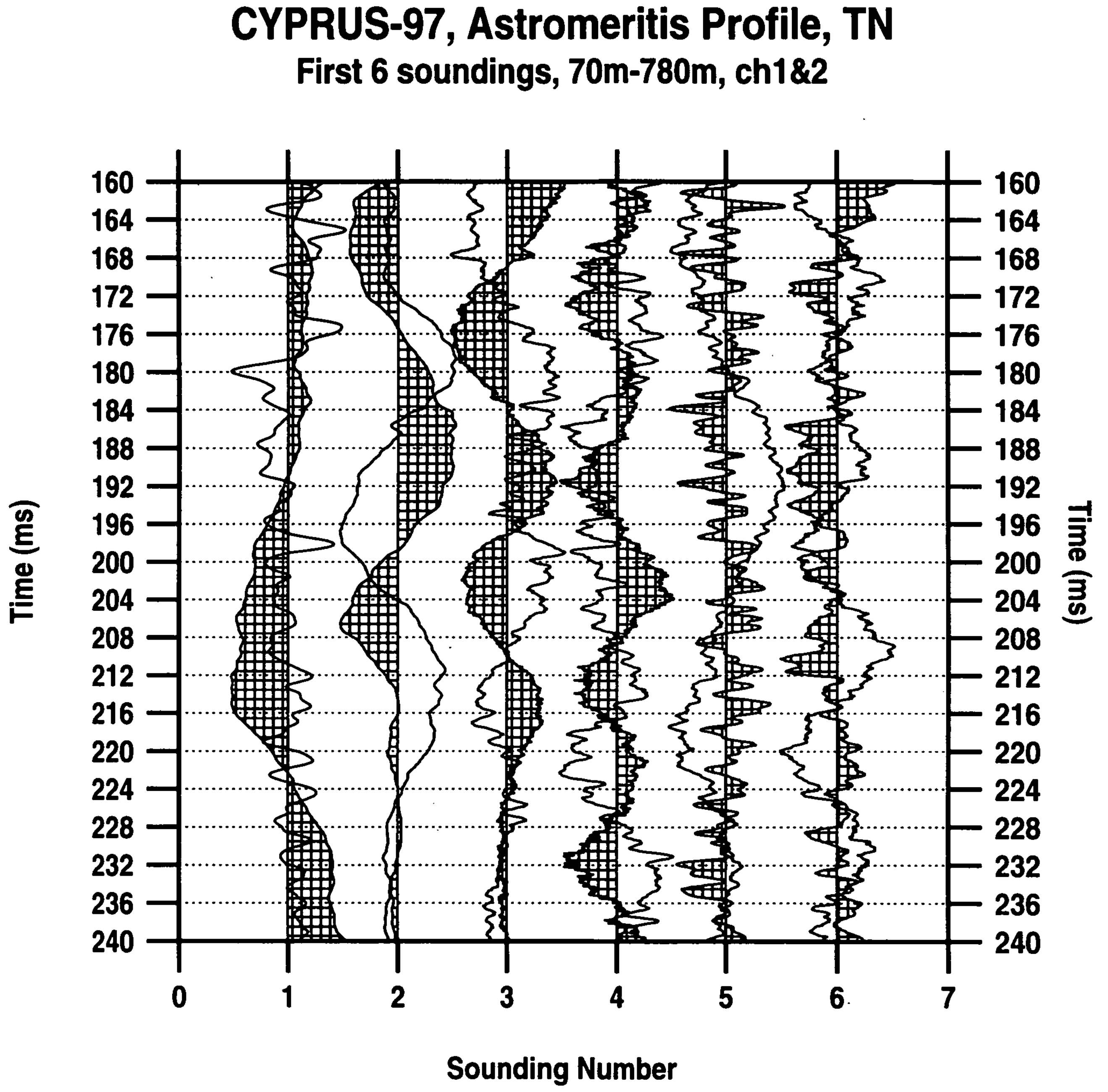

Figure 7.5a Astromeritis profile, second six soundings (960 to 1640 m along profile). Inner two shot-symmetric channels of each sounding (one infill and one line) are overlaid. Trace-normalised data. Time interval 0 to 40 ms.

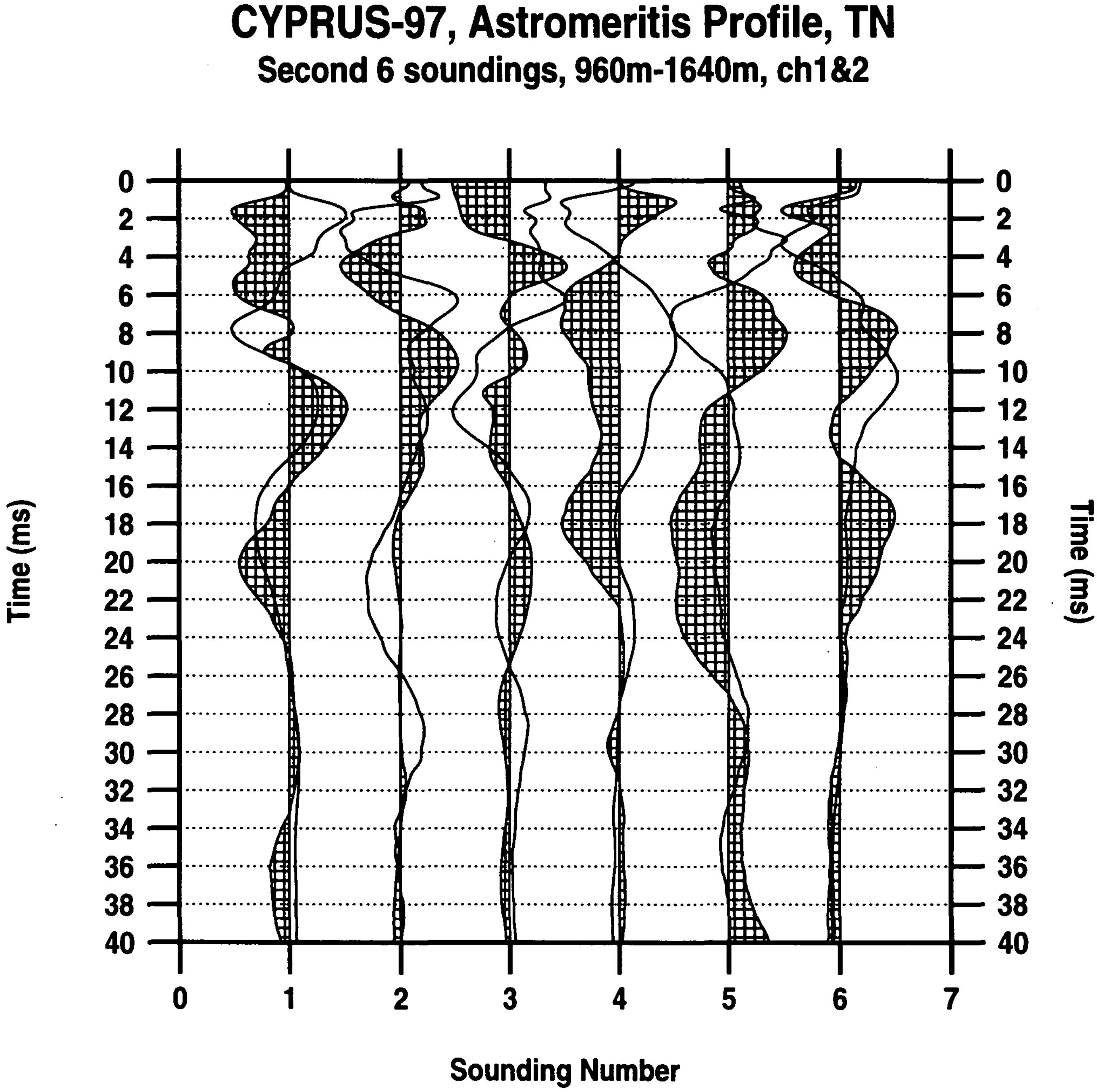

Figure 7.5b Astromeritis profile, second six soundings (960 to 1640 m along profile). Inner two shot-symmetric channels of each sounding (one infill and one line) are overlaid. Trace-normalised data. Time interval 40 to 80 ms.

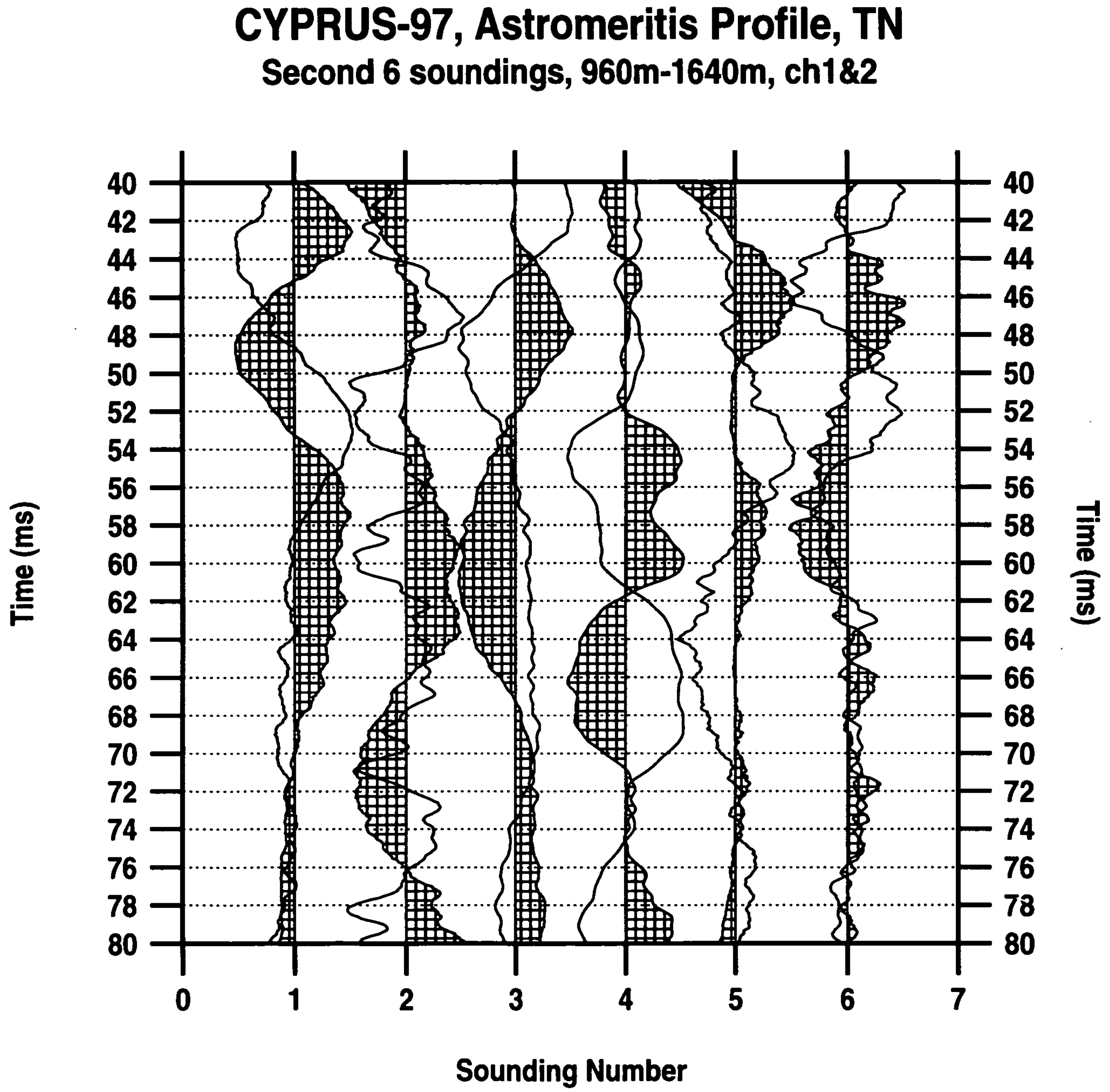

Figure 7.5c Astromeritis profile, second six soundings (960 to 1640 m along profile). Inner two shot-symmetric channels of each sounding (one infill and one line) are overlaid. Trace-normalised data. Time interval 80 to 160 ms.

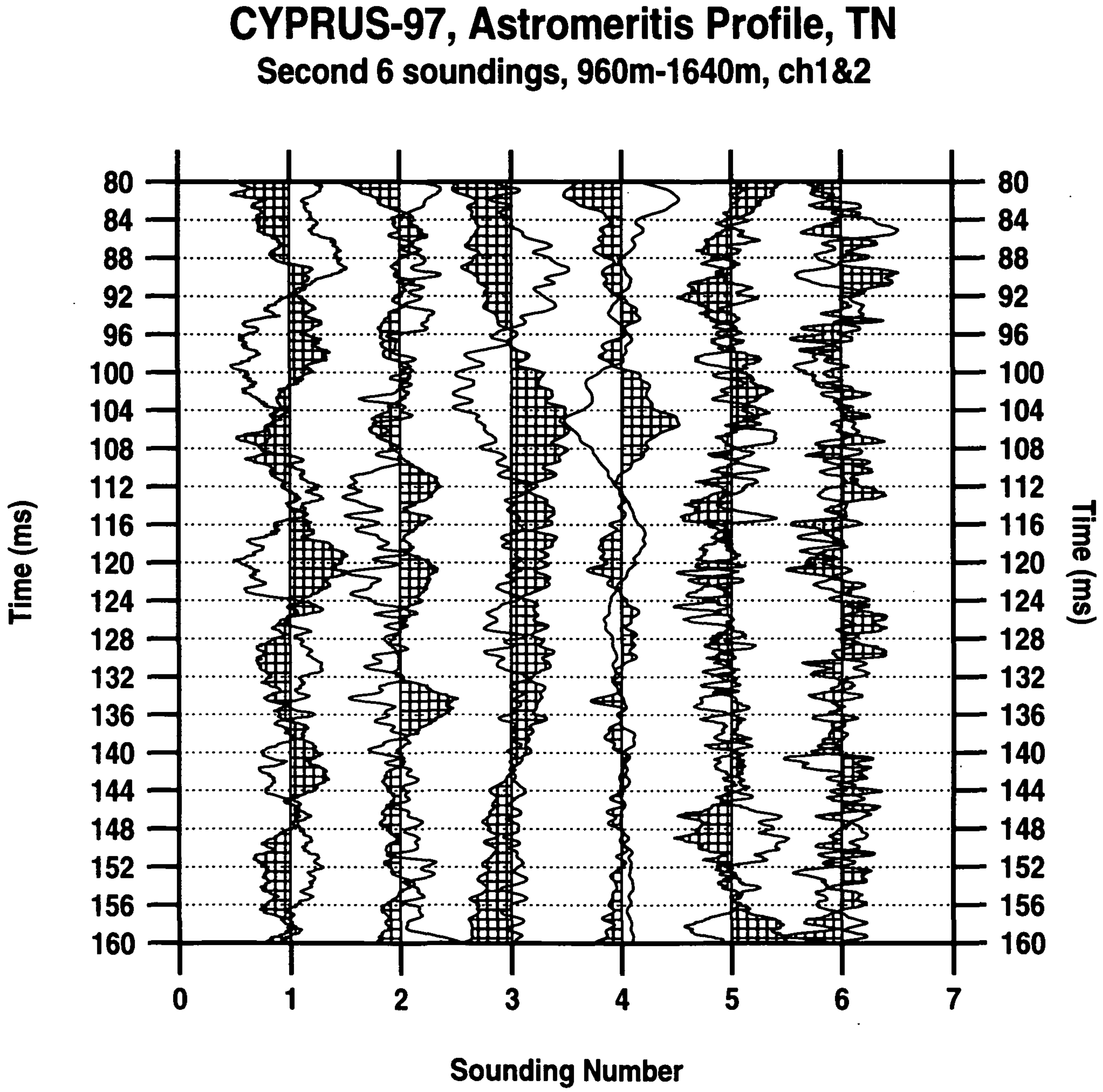

Figure 7.5d Astromeritis profile, second six soundings (960 to 1640 m along profile). Inner two shot-symmetric channels of each sounding (one infill and one line) are overlaid. Trace-normalised data. Time interval 160 to 240 ms.

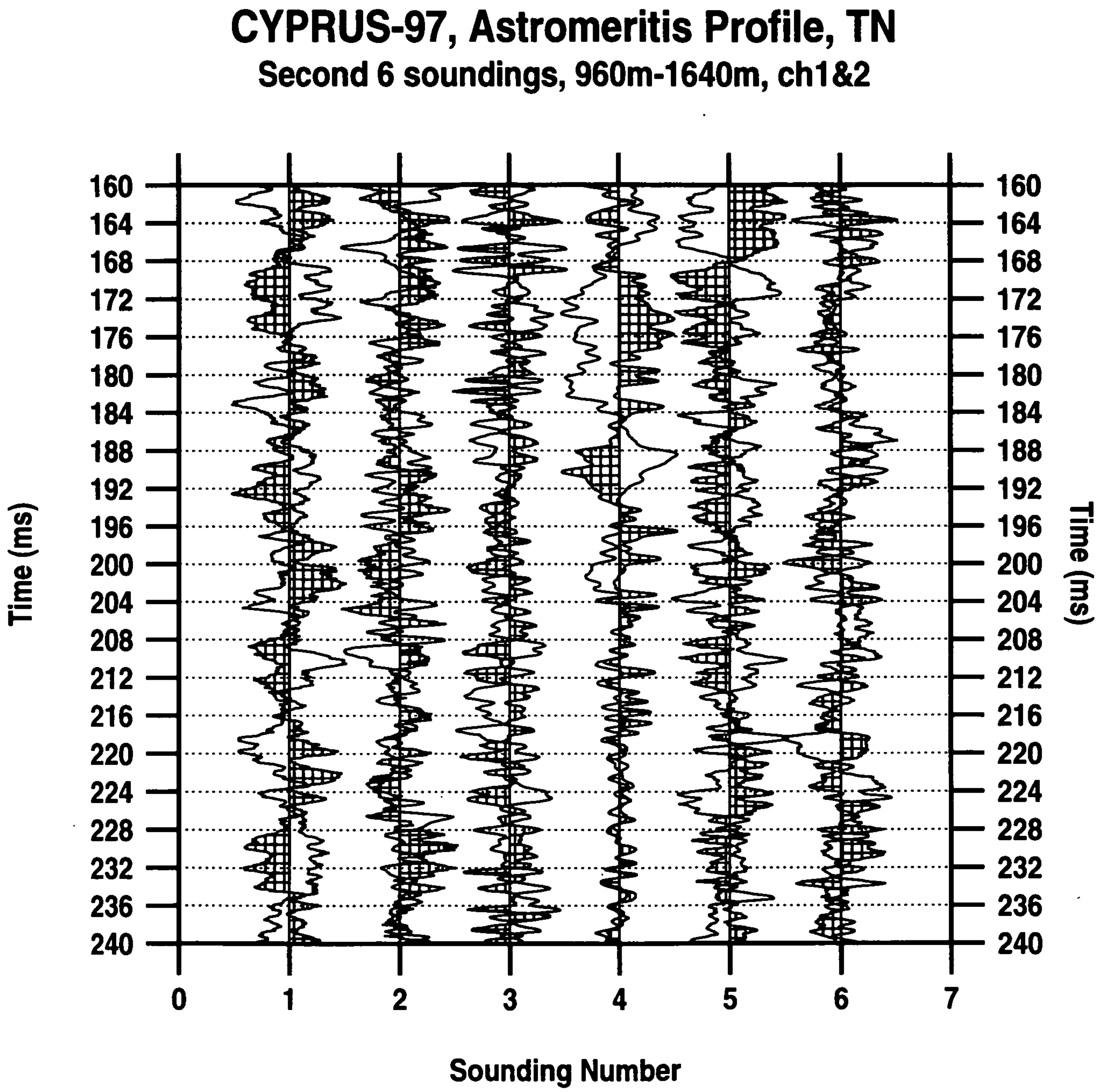

Figure 7.6a Meniko profile, eight soundings (0 to 1210 m along profile). Inner two shot-symmetric channels of each sounding (one infill and one line) are overlaid. Trace-normalised data. Time interval 0 to 40 ms.

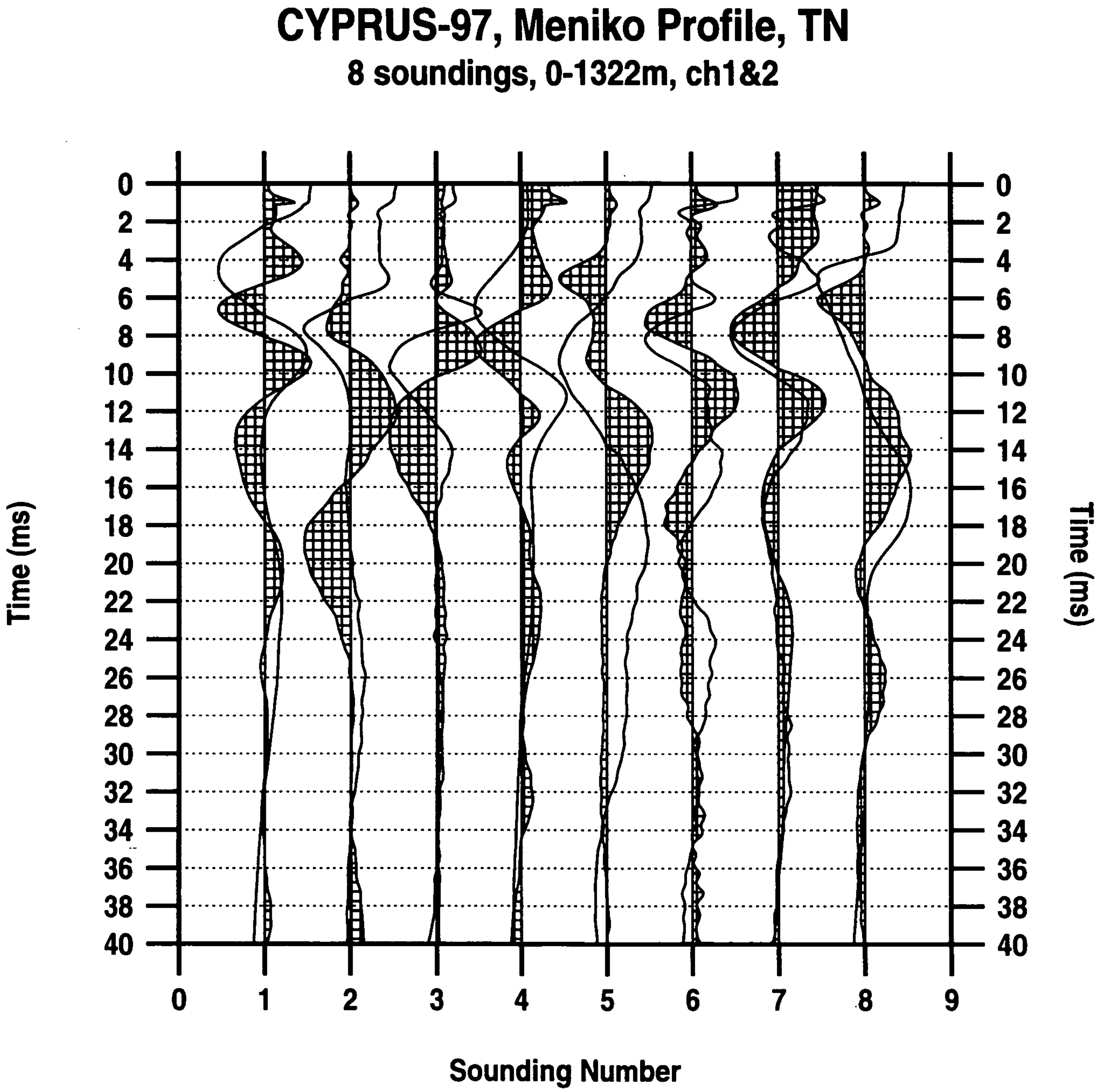

Figure 7.6b Meniko profile, eight soundings (0 to 1210 m along profile). Inner two shot-symmetric channels of each sounding (one infill and one line) are overlaid. Trace-normalised data. Time interval 40 to 80 ms.

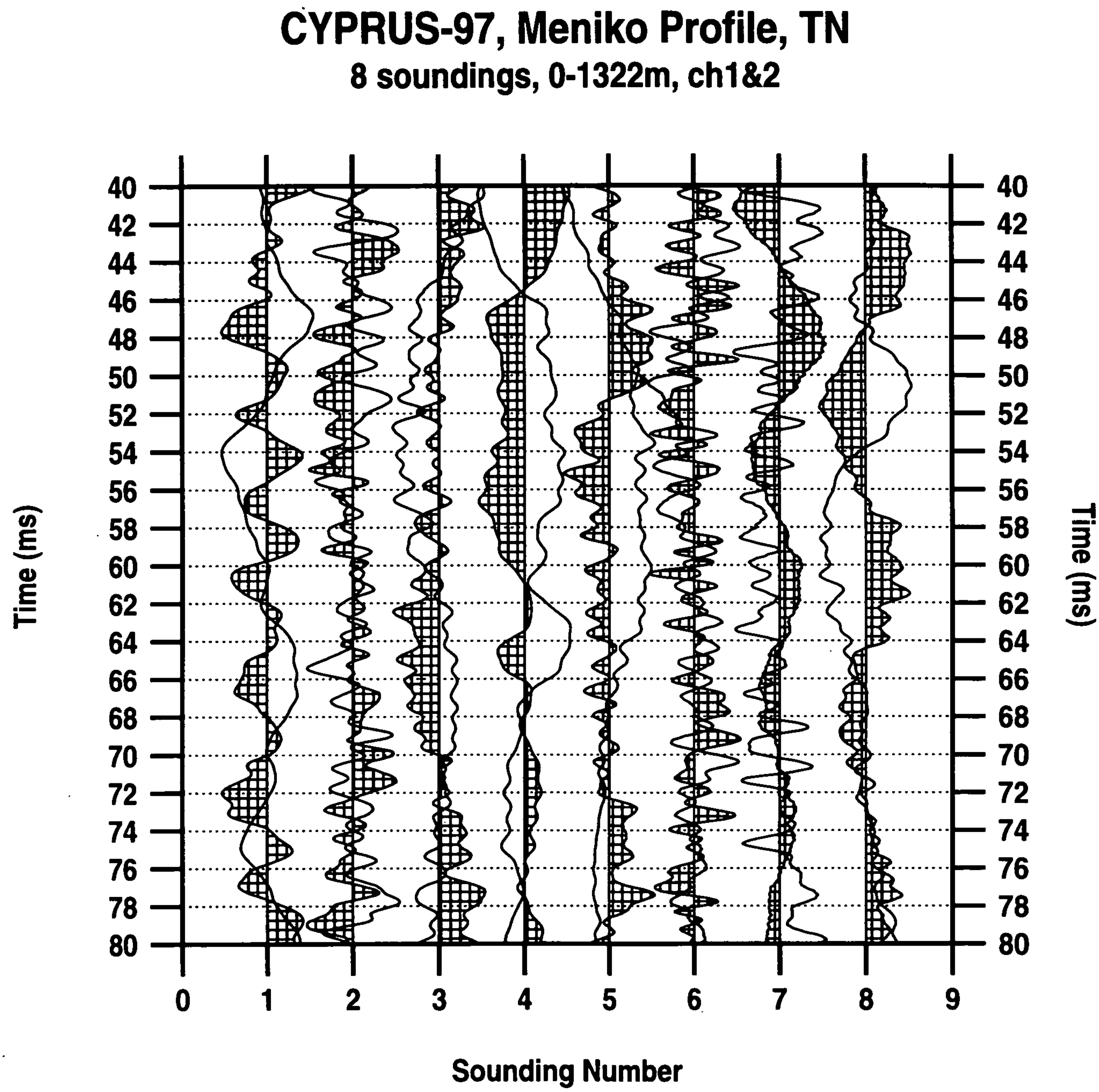

Figure 7.6c Meniko profile, eight soundings (0 to 1210 m along profile). Inner two shot-symmetric channels of each sounding (one infill and one line) are overlaid. Trace-normalised data. Time interval 80 to 160 ms.

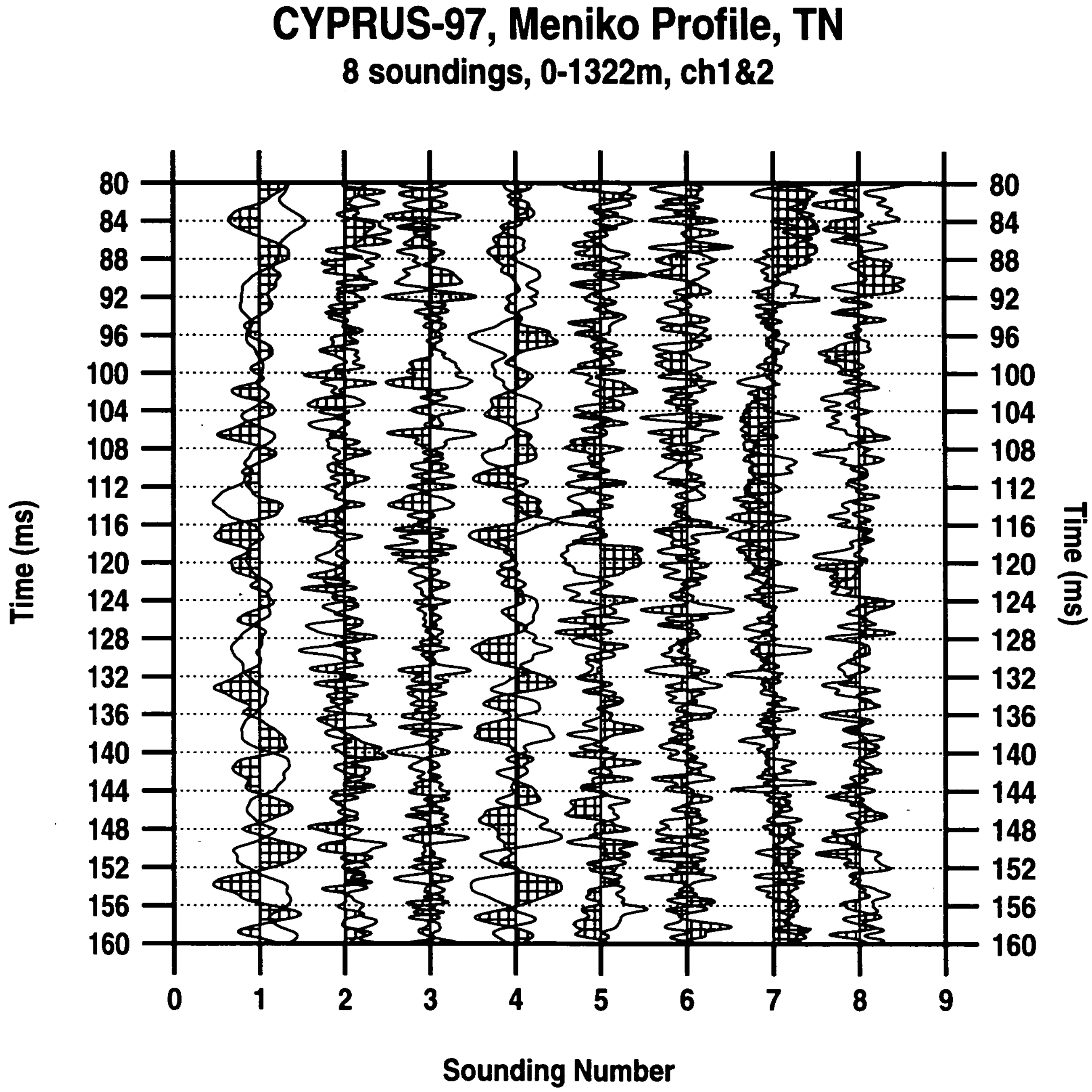

Figure 7.6d Meniko profile, eight soundings (0 to 1210 m along profile). Inner two shot-symmetric channels of each sounding (one infill and one line) are overlaid. Trace-normalised data. Time interval 160 to 240 ms.

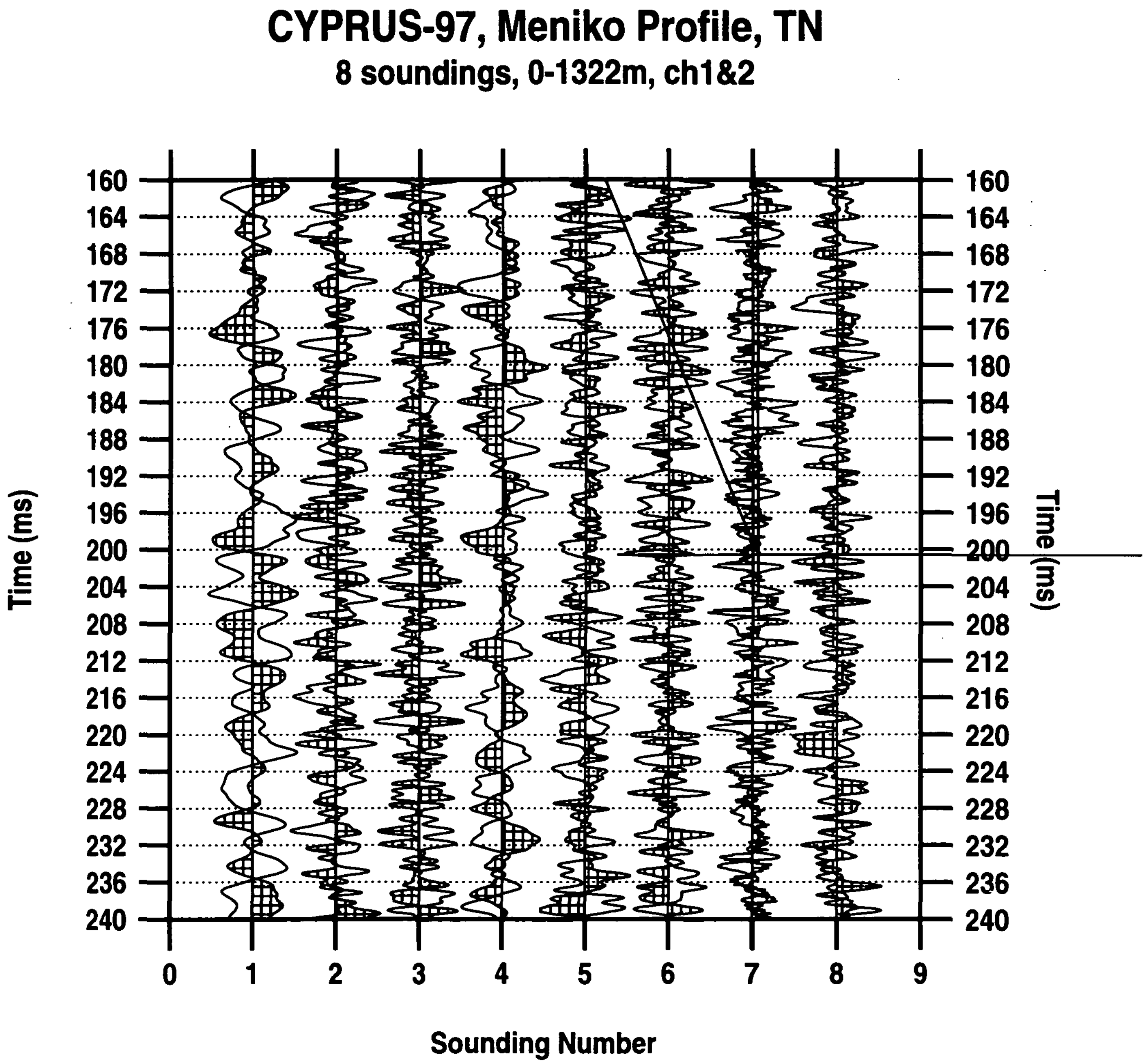

British Geological Survey
Keyworth
Nottingham NG12 5GG

☎ (0115) 936 3100
FAX (0115) 936 3200
WEB www.bgs.ac.uk

Natural Environment Research Council

BGS 1835